Qidan, A. A., Morales-Cespedes, M., García Armada, A. & Elmirghani, J. M. H. (2021). Resource Allocation in User-Centric Optical Wireless Cellular Networks Based on Blind Interference Alignment. *Journal of Lightwave Technology*, 39(21), 6695-6711.

DOI: 10.1109/jlt.2021.3107140

Resource Allocation in User-Centric Optical Wireless Cellular Networks based on Blind Interference Alignment

Ahmad Adnan Qidan, *Member, IEEE,* Máximo Morales-Céspedes, *Member, IEEE,* Ana García Armada, *Senior Member, IEEE* and Jaafar M. H. Elmirghani, *Fellow, IEEE*

***Abstract*—Visible light communications (VLC) have been recently proposed to enhance the capacity of next generation of wireless services. Moreover, VLC networks usually comprise a large number of overlapping optical access points (APs). Moreover, each of these APs provides a small and confined area of coverage in order to generate satisfactory illumination. In this work, a user-centric (UC) clustering formation based on the K-means algorithm is proposed to manage the inter-cell interference (ICI) and enhance the performance of VLC networks. Moreover, assuming that each user is equipped with a reconfigurable photodetector, the use of blind interference alignment (BIA) in each UC cluster is considered. Notice that the data rate demands are not the same for all the users. We formulate an optimization problem to maximize the utility of the network resources allocated to the users based on their demands. After that, a centralized algorithm is proposed to obtain an optimal solution through exhaustive search, which is subject to high complexity. To reduce the complexity of this optimization problem, the problem is divided into sub-problems based on the number of constructed UC clusters. Then, a distributed algorithm via Lagrangian multipliers is proposed within each UC cluster with the aim of providing a near optimal solution to the centralized algorithm. Simulation results demonstrate that the proposed resource allocation algorithms provide higher performance than a uniform resource allocation scheme among users.**

***Index Terms*—Visible light communications, resource allocation, blind interference alignment, user-centric**

I. Introduction

Due to the surge in Internet usage and the need for high speed wireless networks in our daily applications, exploiting new bands beyond the radio frequency (RF) spectrum is required in order to satisfy the demands of the users. Recently, visible light communications (VLC) have been recognized as a promising technology for the next generation of wireless communications [1]–[3]. The light sources such as light emitting diode (LED) lamps can be used for data transmission in addition to their main function of providing illumination. In this sense, light sources do not interfere with other electromagnetic devices, and therefore, VLC can be used in applications that are sensitive to electromagnetic interference such as airplanes, underground mining industry or hospitals [4].

Multiple optical access points (APs) are typically deployed to provide satisfactory illumination and coverage. Each source of light illuminates a small and confined area referred to as *attocell*. As a consequence, VLC networks are subject to inter-cell interference (ICI). Traditional schemes applied to cellular networks for managing the ICI such as frequency reuse (FR) are not suitable for VLC due to the small cell footprint of each optical AP, which might lead to frequency switching every few meters [5]. The network-centric (NC) design proposed in [6]–[9] groups multiple optical APs to generate optical cells with larger coverage so that the ICI can be reduced. This approach obtains fixed-shape cells regardless of the distribution of users or the load balancing among cells. Following the approach based on grouping optical APs, user-centric (UC) designs are derived in [8]–[12] obtaining elastic-shape cells based on the users distribution that adjust better than the NC approach to the requirements of the VLC systems and traffic demands.

Once the optical APs are grouped in cells, multi-user interference (MUI) must be managed. Based on cooperation and channel state information (CSI) at the transmitter side, transmit precoding (TPC) schemes such as minimizing the mean square error (MMSE) [13], zero-forcing (ZF) or interference alignment (IA) [14], [15] have been proposed for maximizing the degrees of freedom (DoF). The DoF can be interpreted as the multiplexing gain or the number of symbols simultaneously transmitted per time slot. Beyond the need for cooperation and CSI at the transmitters, for VLC, transmission through the optical channel involves additional constraints such as ensuring a real and non-negative transmitted signal or the lack of small scale effects, which may generate highly correlated channel responses that hamper the performance of TPC schemes in VLC [16].

A signal processing technique referred to as blind interference alignment (BIA) for aligning the interference without CSI nor cooperation among transmitters is proposed in [17]. Basically, BIA is based on exploiting the channel variations among the users during a set of symbol extensions that com-

Ahmad Adnan Qidan and Jaafar M. H. Elmirghani are with the School of Electronic and Electrical Engineering, University of Leeds, UK (email: {A.A.Qidan, J.M.H.Elmirghani}@leeds.ac.uk).

Máximo Morales-Céspedes and Ana García Armada are with the Department of Signal Theory and Communications, Universidad Carlos III de Madrid, Avda. Universidad 30, 28911, Leganés (Madrid), Spain (email: {maximo, agarcia}@tsc.uc3m.es).

The work of Ahmad Adnan Qidan and Jaafar M. H. Elmirghani has been supported by the Engineering and Physical Sciences Research Council (EPSRC), in part by the INTERNET project under Grant EP/H040536/1, and in part by the STAR project under Grant EP/K016873/1 and in part by the TOWS project under Grant EP/S016570/1. All data are provided in full in the results section of this paper. The work of M. Morales and A. García has been supported by the Spanish National Project TERESA-ADA (TEC2017-90093-C3-2-R) (MINECO/AEI/FEDER, UE) and the project GEOVEOLUZ-CM-UC3M.

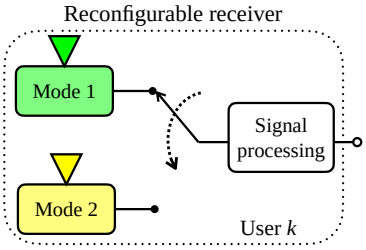

(a) Concept of reconfigurable receiver.

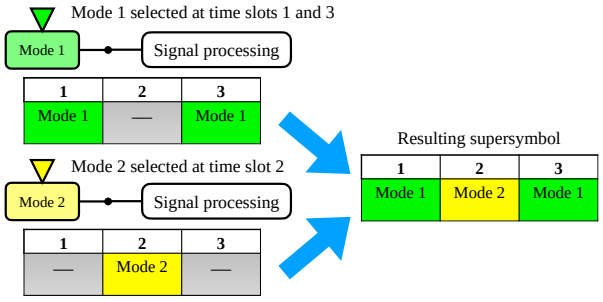

(b) Mode switching. Each mode provides a linearly independent channel response. The switching pattern forms the supersymbol for user k.

Fig. 1. Formation of the supersymbol for a generic user during 3 time slots.

pose a *supersymbol*. These symbol extensions may correspond to frequency or time slots. For the sake of simplicity, each symbol extension corresponds to a time slot from now on. Thus, the implementation of BIA is subject to employing receivers that can switch among a set of channel states that are linearly independent as shown in Fig. 1(a). The supersymbol is composed of the modes selected at each time slot as shown in Fig. 1(b). The concept of reconfigurable photodetector was proposed in [18] to implement BIA schemes in VLC. Basically, a reconfigurable photodetector is composed of several photodiodes whose parameters such as the orientation angle, e.g., following an angle diversity pattern [19], [20], or the filter plus concentrator modify the optical channel response as a non-linear function. Therefore, the reconfigurable photodetector provides a set of linearly independent channel responses to each user. In such a way, a practical implementation of a reconfigurable photodetector is analyzed in [21].

BIA does not require CSIT or cooperation at the transmitter side. It provides other advantages for VLC such as ensuring the non-negativity of the signal without adding a DC bias. It also results in the non-influence of the correlation among the channel responses of the users. Moving to medium-large size VLC networks, BIA schemes are subject to a noise increase proportional to the number of served users and a required coherence time that increases exponentially with the number of served users and optical APs. Furthermore, due to the small and confined area of coverage provided by each optical AP, considering clusters of optical APs for BIA schemes might lead to high ICI. In [8]–[10], [12], alternative BIA schemes are proposed for VLC networks based on exploiting the network topology given by both NC and UC perspectives.

To the best of our knowledge, these BIA-UC approaches do not consider the management of the network resources. Specifically, uniform resource allocation is typically assumed in most of the VLC systems. Therefore, the resource management cannot be adapted to the current heterogeneous traffic demands. The use of utility functions for resource allocation is initially proposed in [22], [23]. A centralized algorithm is proposed in [24] for optimizing the bandwidth allocated to each user, while distributed algorithms are derived in [25], [26] in order to reduce the complexity of the centralized algorithms. Focussing on the resource management in VLC systems, several optimization problems are formulated in [27]–[31] to enhance the performance considering various metrics of VLC networks by allocating power, bandwidth, etc.

In this work, we consider medium-large VLC networks in which BIA schemes are implemented to align the interference among multiple users, each equipped with a reconfigurable photodetector. The main contributions of this work are:

1) Reducing the limitations of BIA schemes for VLC by applying a UC design in which the network is divided into elastic clusters. The K-means algorithm is considered to divide the users into several unique groups. After that, a novel methodology for optical AP association is proposed based on the received optical power.
2) After dividing the whole area into several UC clusters, closed-form expressions for the achievable DoF and user rate are derived considering the implementation of BIA within each cluster as a transmission scheme.
3) Taking into consideration the VLC network topology, an optimization problem for allocating the network resources in order to maximizing their utilization is formulated. To solve this problem, a centralized algorithm is proposed to maximize the overall user rates in the whole area according to the formed clusters.
4) To avoid the high complexity of the centralized algorithm, a distributed algorithm is proposed based on dividing the main problem into several smaller problems given by the number of clusters. Specifically, into each cluster, the users are allowed to request their needs for resources from their corresponding optical APs.

Simulation results show that BIA schemes based on the network topology from a UC perspective (UC-BIA) outperforms TPC and maximum ratio combining (MRC) schemes. In comparison to traditional BIA schemes, i.e., assuming full connectivity and NC approaches (NC-BIA), UC-BIA shows a better performance for VLC networks in terms of achievable user rate and BER. In contrast to our previous works, i.e., [8]–[10], [12], in this work the problem of resource allocation is addressed. It is shown that the proposed resource allocation algorithms provide better performance than uniform resource allocation in the considered scenarios.

The remainder of this paper is organized as follows. In Section II, the system model of the VLC network is described. A brief overview of the implementation of BIA for VLC networks is introduced in Section III. In Section IV, the proposed UC approach is presented, the methodology of BIA schemes is defined, and then, the achievable DoF and user rate for BIA schemes based on the UC approach are derived. The formulation and analysis of the resource allocation problem for both the centralized and distributed algorithms are derived in

Section V. Section VI presents the simulation results. Finally, Section VII provides concluding remarks.

Notation. In the following, we define the notation considered in this work. First, the bold upper case and lower case letters denote matrices and vectors, respectively. All the vectors are defined as column vectors and the transpose operator is applied when required. For representing the identity and zero matrices with $M \times M$ dimension, we call out to the notations $\mathbf{I}_M$ and $\mathbf{0}_M$, respectively, while $\mathbf{0}_{M,N}$ denotes the $M \times N$ zero matrix, $[\,]^T$ and $[\,]^H$ are the transpose and hermitian transpose operators, respectively. Finally, $\mathbb{E}$ is the statistical expectation, and $\mathrm{col}\{\}$ is the column operator that stacks the considered vectors in a column.

II. System Model

We consider a downlink VLC system as shown in Fig. 2, composed of $L, l = \{1, \ldots, L\}$, optical APs providing illumination and data transmission to K, $k = \{1, \ldots, K\}$, users. Each user is equipped with $m = \{1, \ldots, M\}$ photodiodes allocated in an angle diversity pattern while selecting a single photodiode from the M possible photodiodes at time n. This architecture is referred to as reconfigurable photodetector and it is further discussed below. The signal transmitted by the set of L optical APs at time n can be written in vector form as

$$\mathbf{x}[n] = \begin{bmatrix} x_1 & \ldots & x_L \end{bmatrix}^T \in \mathbb{R}_+^{L\times 1}, \tag{1}$$

where x_l is the signal transmitted by optical AP l, which may contain symbols intended to the K users. Thus, the signal received[1] by user k at time n is

$$y^{[k]}[n] = \mathbf{h}^{[k]}\left(m[n]\right)^T \mathbf{x}[n] + z^{[k]}[n], \tag{2}$$

where $\mathbf{h}^{[k]}\left(m[n]\right) \in \mathbb{R}_+^{L\times 1}$ is the channel vector between the L optical APs and user k for preset mode m selected at time n given by

$$\mathbf{h}^{[k]}\left(m[n]\right) = \begin{bmatrix} h_1^{[k]}(m) & \ldots & h_L^{[k]}(m) \end{bmatrix}^T, \tag{3}$$

and $h_l^{[k]}(m)$ is the channel from optical AP l to user k when it selects the m-th photodiode. Moreover, $z^{[k]}[n]$ is real valued additive white Gaussian noise with zero mean and variance σ_z^2 given by the sum of the contributions from both shot noise and thermal noise [32].

The set of optical APs are controlled by a central unit (CU) that provides time synchronization while there is no cooperation for data sharing among them. Besides, CSI is not available at the transmitter side and the CU only knows the topology of the network. Each user selects a specific photodiode at each time slot following a predefined pattern.

A. LED Transmitter

For VLC, the transmitted signal is simultaneously used for providing both constant illumination and data transmission. The maximum level of optical power transmitted by each optical AP is denoted as $P_{\max}$. This power level can provide a high SNR enhancing the performance of VLC networks. Also, a minimum level of irradiated signal power, referred to as $P_{\min}$, must be fulfilled in order to guarantee an acceptable SNR level, which can ensure the required data rate. As a consequence, the transmitted power corresponds to a value within the range $[P_{\min}, P_{\max}]$.

[1]Recall that all the vectors are defined as column vectors and the transpose operator is applied when required.

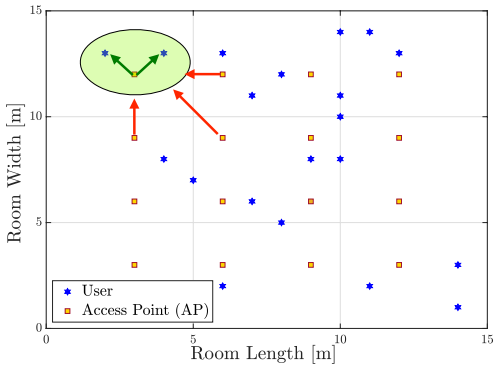

Fig. 2. VLC network composed of a high number of optical APs serving multiple users. The green arrows represent the desired signals, while the red arrows represent the inter-cell interference.

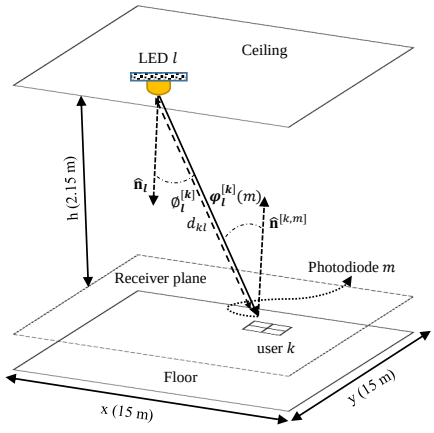

Fig. 3. Geometry of the optical channel model. The LoS component for the optical AP-photodiode pair.

B. Optical Channel Model

The optical channel is composed of a Line-of-Sight (LoS) component, which corresponds to the direct link between transmitter and user, and a Non-LoS (NLoS) component caused by the reflection on walls, ceiling, floor and other elements of the scenario. According to [33], the LoS component represents the largest portion of the received optical power. Moreover, recall that, each user is equipped with a reconfigurable photodetector composed of M, $m = \{1, \ldots, M\}$, each providing a preset mode by pointing out to a specific orientation, and therefore, generating a wide field of view (FoV) [18]. Therefore, LoS propagation is guaranteed to constitute the most important contribution of the optical channel. Thus, the NLoS component can be neglected.

The LoS component is determined by the geometry of the transmitter-receiver pair as shown in Fig. 3. The distance between optical AP l and user k is denoted as d_{kl} and

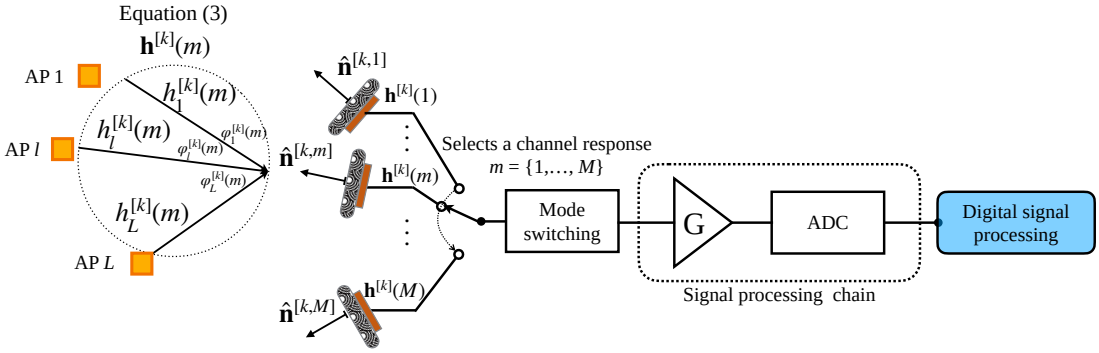

Fig. 4. Architecture of the reconfigurable photodetector. The channel responses from the L optical APs are received by each of the M photodiodes of user k that are allocated in an angle diversity, i.e., with a distinct orientation vector each. Then, a specific channel response $\mathbf{h}^{[k]}(m)$, namely preset mode, is selected by connecting a unique photodiode with the single signal processing chain.

the irradiance[2] and incidence angles for preset mode m are denoted as $\phi_l^{[k]}$ and $\varphi_l^{[k]}(m)$, respectively. Thus, the LoS optical channel between user k and AP l at preset mode m is given by [33]

$$h_{l,\mathrm{LoS}}^{[k]}(m) = \begin{cases} \dfrac{\epsilon A_{pd}}{d_{kl}^2} R_0\left(\phi_l^{[k]}\right) g\left(\varphi_l^{[k]}(m)\right) \cos^r\left(\varphi_l^{[k]}(m)\right), & \varphi_l^{[k]} \leq \Psi_F \\ 0, & \varphi_l^{[k]} \geq \Psi_F, \end{cases} \tag{4}$$

where ϵ and A_{pd} are the responsivity and detection area of the photodiode[3], respectively. Moreover, $R_0\left(\phi_l^{[k]}\right)$ denotes the Lambertian radiation intensity, which is given by $R_0 = \frac{t+1}{2\pi}\cos^t\left(\phi_l^{[k]}\right)$, where $t = \frac{-\ln 2}{\ln(\cos(\phi_{1/2}))}$ is the Lambertian emission and $\phi_{1/2}$ is the transmitter semiangle. Furthermore, $g\left(\varphi_l^{[k]}(m)\right)$ is the gain of optical filter and concentrator, r is the coefficient of photodiode and Ψ_F denotes the FoV of the photodiode.

C. Reconfigurable photodetector

The purpose of the reconfigurable photodetector is to provide M linearly independent channel vectors (see (3)) to user k. That is, $\mathbf{h}^{[k]}(m) \neq a \cdot \mathbf{h}^{[k]}(m') + b$, $m = 1, \ldots, M$, $a, b \in \mathbb{R}$. To do that, the M photodiodes of user k are allocated following a geometrical pattern that provides diversity [19]. Notice that this approach generates a distinct incidence angle at each photodiode of user k, which has a direct impact on a non-linear function such as the cosine in the channel response as can be seen in (4). In [20], the photodiodes are allocated around the faces of a hand-held device to generate this angle diversity. In such a way, the use of lenses at each photodiode can be also employed for this purposes so that the filter plus concentrator gain in (3) is not a linear function [18].

Assuming photodiodes are allocated according to an angle diversity pattern, the orientation of photodiode m of user k is given by its azimuth and elevation angles, which are denoted by $\alpha^{[k,m]}$ and $\theta^{[k,m]}$, respectively. Thus, the orientation angle of photodiode m of user k is defined as

$$\hat{\mathbf{n}}^{[k,m]} = \Big[\sin\left(\theta^{[k,m]}\right)\cos\left(\alpha^{[k,m]}\right), \sin\left(\theta^{[k,m]}\right)\sin\left(\alpha^{[k,m]}\right), \cos\left(\theta^{[k,m]}\right)\Big], \tag{5}$$

Then, the irradiance angle is given by the position of each optical AP l and user k, which define the vector $\mathbf{v}_l^{[k]}$ steering from optical AP l to user k, while the incidence angle is determined by these parameters and also by the orientation of photodiode m of user k. Assuming that the optical APs are pointing to the floor, i.e., their orientation angle is $\hat{\mathbf{n}}_l = [0, 0, -1]$, the irradiance and incidence angles are given by

$$\phi_l^{[k]} = \arccos\left(\frac{\hat{\mathbf{n}}_l \cdot \mathbf{v}_l^{[k]}}{\|\hat{\mathbf{n}}_l\|\|\mathbf{v}_l^{[k]}\|}\right) \tag{6}$$

and

$$\varphi_l^{[k]}(m) = \arccos\left(\frac{\hat{\mathbf{n}}^{[k,m]} \cdot \mathbf{v}_l^{[k]}}{\|\hat{\mathbf{n}}^{[k,m]}\|\|\mathbf{v}_l^{[k]}\|}\right), \tag{7}$$

respectively. Notice that each photodiode m provides a distinct incidence angle to user k, which affects the channel response (see (4)) in a non-linear fashion. Therefore, generating linearly independent channels among the M photodiodes of user k, which are referred to as preset modes of the reconfigurable photodetector.

Once the set of linearly independent channel responses is obtained, a unique channel response, i.e., a preset mode, is connected to a single signal processing chain through a selector that switches among the available preset modes of the reconfigurable photodetector as shown in Fig. 4. It is assumed that the speed of switching is enough to select a specific preset mode every time slot. Although the electronic components can satisfy this requirement nowadays, alternative schemes such as [34] can be applied for slower speed of switching. Moreover, this receiver architecture allows us to reduce the complexity and energy consumption since a single cascade of amplifiers is used. These can include a transimpedance amplifier, post-amplifiers to adapt the signal, control gain, etc., and a single analog-to-digital converter (ADC).

[2]The distance among the photodiodes of user k is much smaller than the distance from any of these photodiodes to any optical AP. Therefore, the irradiance angle between the photodiode m of user k and optical AP l, can be approximated as $\phi_l^{[k]}(m) \approx \phi_l^{[k]}$.

[3]The same responsivity and area of detection are considered for all the photodiodes that compose the reconfigurable photodetector.

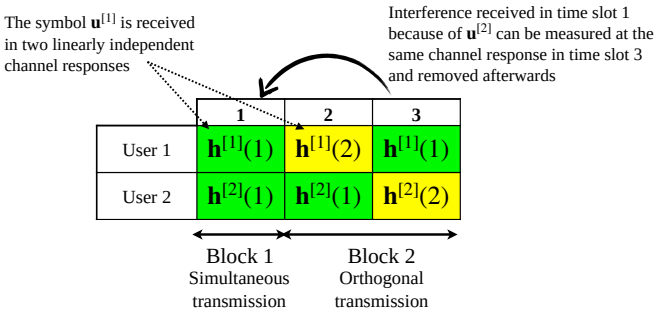

Fig. 5. BIA supersymbol for the MISO BC scenario with $L = 2$ optical APs and $K = 2$ users. Each color represents a preset mode. The procedure to decode the symbol $\mathbf{u}^{[1]}$ by user 1 is commented in detail.

III. Implementation of BIA for VLC networks

BIA is a transmission scheme firstly proposed in [17].It considers a predefined pattern of channel modes selected by each user during a set of time slots (see Fig. 1). It uses these modes to remove the interference because of transmission to other users by measuring that interference and subtracting it afterwards exploiting a particular structure of these patterns without the need for CSI or cooperation among transmitters. In this sense, BIA outperforms the DoF achieved by orthogonal transmission schemes, which are limited to 1 DoF per time slot. Indeed, in [35], it is demonstrated that the DoF achieved by BIA corresponds to the optimal value in the absence of CSI at the transmitters. Thus, motivated by the concept of reconfigurable photodetectors we focus on the implementation of BIA in VLC networks. In the following, the principles of BIA are introduced for a simple VLC network, and then, the general case is considered.

1) Toy example: For illustration purposes, we consider a VLC network comprising $L = 2$ optical APs serving $K = 2$ users able to switch between 2 preset modes. Hence, the proposed scenario corresponds to a multiple-input single output broadcast channel (MISO BC). For this case, the switching patterns carried out by both users form a supersymbol that comprises 3 time slots, as shown in Fig. 5. The transmitted signal during the 3 time slots of the supersymbol follow the structure described in Table I, which can be written as

$$\mathbf{X} = \begin{bmatrix}\mathbf{x}[1]\\ \mathbf{x}[2]\\ \mathbf{x}[3]\end{bmatrix} = \begin{bmatrix}\mathbf{I_2}\\ \mathbf{I_2}\\ \mathbf{0_2}\end{bmatrix}\mathbf{u}^{[1]} + \begin{bmatrix}\mathbf{I_2}\\ \mathbf{0_2}\\ \mathbf{I_2}\end{bmatrix}\mathbf{u}^{[2]}, \tag{8}$$

where $\mathbf{x}[n] \in \mathbb{R}_+^{L\times 1}$, $L = 2$, is the signal transmitted during time slot n, $\mathbf{I_2}$ and $\mathbf{0_2}$ are 2×2 identity and zero matrices, respectively, and $\mathbf{u}^{[k]} = [u_1^{[k]}, u_2^{[k]}] \in \mathbb{R}_+^{L\times 1}$ is the desired symbol, which contains 2 DoF intended to user k each, and $u_l^{[k]}$ is the symbol transmitted by optical AP l. Notice that simultaneous transmission to both users occurs in the first time slot, and therefore, the received signal is polluted by interference due to transmission to other user. On the other hand, the symbols $\mathbf{u}^{[1]}$ and $\mathbf{u}^{[2]}$, which carry 2 DoF each, are transmitted orthogonally, i.e., free of interference, in time slots 2 and 3, respectively. It is worth remarking that pure orthogonal transmission achieves 1 DoF per channel use, i.e., 3 DoF during the 3 time slots of the supersymbol, while the proposed BIA scheme transmits 4 DoF during the same supersymbol length.

TABLE I
Transmitted signal for $L = 2$ and $K = 2$

	AP 1	AP 2
Time slot 1	$u_1^{[1]} + u_1^{[2]}$	$u_2^{[1]} + u_2^{[2]}$
Time slot 2	$u_1^{[1]}$	$u_2^{[1]}$
Time slot 3	$u_1^{[2]}$	$u_2^{[2]}$

BIA is based on generating *alignment blocks* in which the channel state of a specific user varies among L linearly independent channel responses while the state of all other users remains constant. For the considered toy example a single alignment block is allocated to each user. Specifically, the time slots $\{1, 2\}$ and $\{1, 3\}$ form an alignment block for users 1 and 2, respectively. Focussing on user 1 without loss of generality, the optical APs transmit the symbol $\mathbf{u}^{[1]}$ during time slots $\{1, 2\}$. Notice that, the reconfigurable photodetector of user 1 switches between two distinct preset modes during these time slots providing linearly independent channel responses. On the other hand, user 2 maintains a fixed preset mode during the time slots $\{1, 2\}$ in order to align the interference. The signal received by user 1 is expressed as

$$\begin{bmatrix}y^{[1]}[1]\\ y^{[1]}[2]\\ y^{[1]}[3]\end{bmatrix} = \underbrace{\begin{bmatrix}\mathbf{h}^{[1]}(1)^T\\ \mathbf{h}^{[1]}(2)^T\\ \mathbf{0_{2,1}}^T\end{bmatrix}}_{\text{rank=2}}\mathbf{u}^{[1]} + \underbrace{\begin{bmatrix}\mathbf{h}^{[1]}(1)^T\\ \mathbf{0_{2,1}}^T\\ \mathbf{h}^{[1]}(2)^T\end{bmatrix}}_{\text{rank=1}}\mathbf{u}^{[2]} + \begin{bmatrix}z^{[1]}[1]\\ z^{[1]}[2]\\ z^{[1]}[3]\end{bmatrix}. \tag{9}$$

Notice that, the interference is aligned into a 1-rank matrix over a vector $\begin{bmatrix}1 & 0 & 1\end{bmatrix}^T$, while the desired symbol $\mathbf{u}_\zeta^{[1]}$ appears through a 2-rank matrix over a vector $\begin{bmatrix}1 & 1 & 0\end{bmatrix}^T$. Moreover, the symbols $\mathbf{u}^{[1]}$ and $\mathbf{u}^{[2]}$ are transmitted in orthogonal fashion during the second and third time slots, respectively. Still focussing on user 1, the interference received due to the transmission of $\mathbf{u}^{[2]}$ in the first time slot can be measured at the third time slot, and then, subtracted afterwards. Thus, the received signal after interference subtraction can be expressed as

$$\begin{bmatrix}y^{[1]}[1] - y^{[1]}[3]\\ y^{[1]}[2]\end{bmatrix} = \underbrace{\begin{bmatrix}\mathbf{h}^{[1]}(1)^T\\ \mathbf{h}^{[1]}(2)^T\end{bmatrix}}_{\mathbf{H}^{[1]}}\mathbf{u}_\zeta^{[1]} + \begin{bmatrix}z^{[1]}[1] - z^{[1]}[3]\\ z^{[1]}[2]\end{bmatrix}. \tag{10}$$

In (10), the channel responses $\mathbf{h}^{[1]}(1)$ and $\mathbf{h}^{[1]}(2)$ are linearly independent since they correspond to different preset modes provided by the reconfigurable photodetector of user 1. This condition is required to form a 2-rank matrix so that the 2 DoF in symbol $\mathbf{u}^{[1]}$ can be decoded by solving the problem (10), i.e., 2/3 DoF can be achieved during the entire supersymbol for user 1. Following the same procedure, user 2 can decode the 2 DoF in $\mathbf{u}^{[2]}$ transmitted over the time slots $\{1, 3\}$ while measuring the interference received due to the transmission to user 1 at second time slot. As a result, 4/3 DoF per time slot can be achieved for $L = 2$ optical APs serving $K = 2$ users scenario based on the BIA scheme,

which outperforms the 1 DoF per time slot achievable by pure orthogonal transmission.

2) General case: The supersymbol of BIA for MISO BC VLC networks, which comprises L optical APs serving K users, must contain $\zeta = \{1, \ldots, (L-1)^{K-1}\}$ alignment blocks allocated to each user satisfying the following conditions:

- **Ensuring the decodability of each symbol.** Solving the L DoF contained in each symbol intended to user k, which is denoted by $\mathbf{u}_{\zeta}^{[k]}$ for the ζ-th alignment block that requires at least L linearly independent channel responses (see (10) for $L = 2$). Thus, the reconfigurable photodetector of user k must switch among L preset modes within the transmission of the $\zeta-$th alignment block in which transmission of $\mathbf{u}_{\zeta}^{[k]}$ occurs.
- **Alignment of the interference.** BIA is based on measuring the interference that transmission in each alignment block of symbol $\mathbf{u}_{\zeta}^{[k]}$, causes in all other users. To do that, the reconfigurable photodetector of user $k^{'}$, $k^{'} \neq k$, must remain in a constant preset mode during each alignment block of user k. Therefore, the interference is aligned in less dimensions than the symbol intended to user k. For instance, in the supersymbol shown in Fig. 5, user 2 maintains the preset mode 1 during the alignment block of user 1, which comprises the time slots $\{1, 2\}$.

Following [17], the supersymbol of the BIA scheme is divided into two blocks denoted as Block 1 and Block 2. In Block 1, transmission to K users is carried out simultaneously, and therefore, each user is subject to interference due to transmission to all other $K-1$ users. Specifically, Block 1 consists of the first $(L-1)$ time slots of each alignment block of each user. These time slots can be defined as a group, and each group belongs to one alignment block. As a consequence, Block 1 consists of a total of $(L-1)^{K-1}$ groups allocated to each user. Therefore, the length of Block 1 comprises $(L-1)\times(L-1)^{K-1} = (L-1)^{K}$ time slots as is shown in Fig. 6. On the other hand, Block 2 comprises the last time slot of each alignment block of each user with the aim of transmitting the information to all users in orthogonal fashion. Therefore, the length of Block 2 is equal to $K(L-1)^{K-1}$ time slots. This structure of the supersymbol can be used to measure the interference due to the simultaneous transmission, which is carried out over Block 1, through Block 2 and subtract it afterwards. More details about BIA are described in [17].

Finally, each of the K users is able to decode L DoF in each of its $(L-1)^{K-1}$ alignment blocks over a supersymbol that comprises $(L-1)^{K}+K(L-1)^{K-1}$ time slots, i.e., $(L-1)^{K}$ time slots of Block 1 plus $K(L-1)^{K-1}$ time slots of Block 2. Thus, the normalized sum-DoF based on the BIA scheme is given by

$$\mathrm{DoF} = \frac{LK(L-1)^{K-1}}{(L-1)^{K}+K(L-1)^{K-1}} = \frac{LK}{L+K-1}. \quad (11)$$

This value can be achieved by solving the symbols received during the alignment blocks of each user. Without loss of generality, the received signal after interference subtraction over an alignment block ζ of user k can be written as

$$\tilde{\mathbf{y}}^{[k]} = \underbrace{\begin{bmatrix} \mathbf{h}^{[k]}(1)^{T} \\ \vdots \\ \mathbf{h}^{[k]}(L-1)^{T} \\ \mathbf{h}^{[k]}(L)^{T} \end{bmatrix}}_{\mathbf{H}^{[k]}} \mathbf{u}_{\zeta}^{[k]} + \begin{bmatrix} z^{[k]}[1] - \sum_{k' \neq k}^{K} z^{[k]}[\tau] \\ \vdots \\ z^{[k]}[L-1] - \sum_{k' \neq k}^{K} z^{[k]}[\tau] \\ z^{[k]}[L] \end{bmatrix}, \quad (12)$$

where $\tilde{\mathbf{y}}^{[k]} \in \mathbb{R}_{+}^{L\times 1}$, $\mathbf{u}_{\zeta}^{[k]} = \left[u_{\zeta,1}^{[k]}, \ldots, u_{\zeta,L}^{[k]}\right]^{T}$ and the temporal index refers to the position in the alignment block rather than the corresponding temporal index within the supersymbol for the sake of simplicity. Note that, in (12), the symbol $\mathbf{u}_{\zeta}^{[k]}$ containing L DoF is received along L distinct preset modes of the reconfigurable photodetector of user k. Thus, the channel matrix $\mathbf{H}^{[k]}$ exclusively depends on the channel responses provided by the reconfigurable photodetector of user k, and it is defined as

$$\mathbf{H}^{[k]} = \begin{bmatrix} \mathbf{h}^{[k]}(1) & \ldots & \mathbf{h}^{[k]}(L) \end{bmatrix}^{T} \in \mathbb{R}^{L\times L}, \quad (13)$$

which corresponds to a full-rank matrix and allows us to decode the L DoF contained in $\mathbf{u}_{\zeta}^{[k]}$ successfully. Thus, the achievable user rate for user k is given by

$$r^{[k]} = \frac{1}{L+K-1}\log_2\left(\mathbf{I} + P_{\mathrm{str}}\mathbf{H}^{[k]}{\mathbf{H}^{[k]}}^{H}{\mathbf{R}_z}^{-1}\right), \quad (14)$$

where P_{str} is the optical power allocated to each stream, $\mathbf{H}^{[k]} = \begin{bmatrix} \mathbf{h}^{[k]}(1) & \ldots & \mathbf{h}^{[k]}(L) \end{bmatrix}^{T} \in \mathbb{R}^{L\times L}$ is the channel matrix of user k, and $\mathbf{R}_z = \begin{bmatrix} K\mathbf{I}_{L-1} & 0 \\ 0 & 1 \end{bmatrix}$.

Beyond the absence of CSI at the transmitters and the lack of cooperation, BIA offers several advantages for VLC networks. Only some synchronization is required since each optical AP transmits the symbols $u_{\zeta,l}^{[k]}$ that collectively compose the symbol $\mathbf{u}_{\zeta}^{[k]}$ (see (8) and (12)). Also, the transmitted signal is naturally real and non-negative since the precoding matrices are composed of $\{0, 1\}$ values for BIA (see (8)) and the achievable rate does not depend on the correlation among channel responses of the users; it only depends on the channel responses generated by the preset modes of each user (see (12)).

It is interesting to remark that there exists a trade-off between DoF and achievable rate. As the number of users increases, the achievable DoF tends to L (see (11) as K tends to infinity). That is, the same DoF as the theoretically is achievable in a multiple-input multiple-output channel with L transmitters and K users, which is given by $\min(L, K)$. On the other hand, a noise enhancement occurs and is proportional to the number of users in the first $K-1$ slots of (12), and that the physical channel must remain constant during the entire supersymbol so that the resulting channel of each user only depends on the selected preset mode. This trade-off motivates the use of UC clustering and resource allocation for VLC networks based on BIA as proposed in this work. Moreover, it is worth noticing that in contrast to TPC schemes such as [13]–

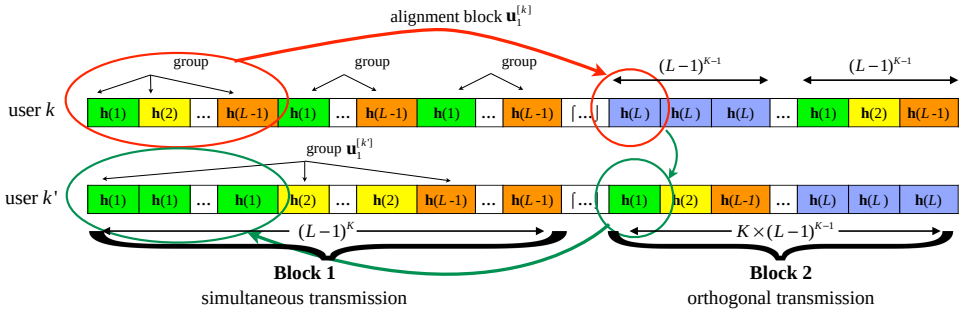

Fig. 6. BIA supersymbol for MISO BC general case with L optical APs serving K users. Notice that, the first $(L-1)$ time slots of each alignment bock belong to Block 1, while the last time slot belongs to Block 2. The interference that the transmission of $\mathbf{u}_1^{[k]}$ generates at user k' can be measured in Block 2 and subtracted afterwards. Each color represents a preset mode.

[15], the methodology for constructing the BIA scheme does not change if the number of users is greater than the number of optical APs.

IV. User Centric Cluster Formation (UC)

For indoor VLC environments composed of multiple optical APs, the performance might be degraded due to the interference at the cells edges. The most straightforward way to avoid the interference based on BIA schemes is to simply assume a fully connected design, i.e., considering a setting where all users are connected to the whole set of optical APs. However, in addition to the fact that achieving full connectivity is unlikely for VLC systems due to the small and confined area of coverage provided by each optical AP, this approach leads to a considerable noise enhancement proportional to the number of served users and a large supersymbol length, i.e., a large required coherence time.

In this context, a feasible solution for managing the ICI in BIA schemes applied to VLC networks is required. The formation of some prespecified clusters can minimize the ICI where multiple neighboring optical APs are merged to form several NC clusters. These clusters are formed with fixed shapes regardless of the distribution of users. It is worth mentioning that the network topology from the NC perspective eliminates only a fraction of the ICI where the users at the edge of each cluster are still subject to the interference received from the neighboring clusters. To circumvent this, a UC approach was proposed in [8], [11] to form clusters based on the distribution of users. That is, the clusters are formed with elastic shapes and change over time based on the updates in the network topology.

For illustrative purposes, let us consider a simple toy example comprising $L = 4$ optical APs and $K = 4$ users as is shown in Fig. 7. In Fig. 7(a), each user is connected to its corresponding optical AP while receiving interference due to the LoS components of the neighbouring optical APs. In Fig. 7(b), the full connectivity BIA approach is implemented, and therefore, it is assumed that each user receives a useful signal from all optical APs at the cost of increasing the noise and the required coherence time. On the other hand, a NC approach is considered in Fig. 7(c), where two static clusters are constructed, each comprising 2 optical APs serving 2 users. In this sense, an orthogonal resource allocation scheme must

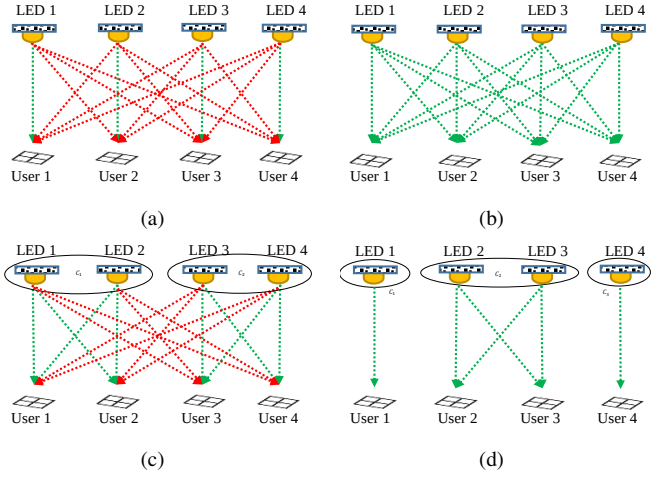

Fig. 7. (a) Each user is served by its corresponding optical AP and receives interference from the neighboring optical APs. (b) Full connectivity is assumed. (c) Two static clusters are constructed with interference at the clusters edges. (d) Three elastic clusters are constructed and the ICI is avoided.

be considered to avoid the interference represented by the red links between the NC clusters. Finally, the UC approach is implemented, and 3 UC clusters are constructed as is shown in Fig. 7(d). These clusters are characterized by their irregular shapes and change in a dynamic fashion with the distribution of users so that the ICI can be minimized and even neglected.

In the following, we present UC cluster formation for VLC based on BIA schemes. First, we carry out the user set formation, and then, the corresponding optical APs for each cluster is determined. Finally, the achievable DoF and user rate are derived taking into consideration the UC approach.

A. UC clustering

Let us first introduce some useful notations before presenting the construction of the UC clusters. The K-means algorithm initially derived in [36] is considered under a given number of clusters denoted as C, $c = \{1, \ldots, C\}$, which is defined as a set hosting all the constructed clusters. Moreover, each UC cluster is denoted by C_c and is constituted by two subsets; the users subset denoted by $\mathcal{V}_{\mathcal{K}_c}$ and the optical APs subset denoted by $\mathcal{V}_{\mathcal{L}_c}$. It is assumed that each cluster C_c is

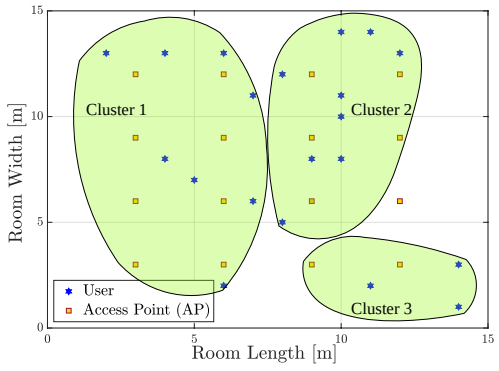

Fig. 8. Cluster formation from the UC perspective assuming $C = 3$ based on the K-means algorithm.

formed by a unique users subset as well as a unique optical APs subset, i.e.,

$$C_c = \mathcal{V}_{\mathcal{L}_c} \cup \mathcal{V}_{\mathcal{K}_c}, \mathcal{V}_{\mathcal{L}_c} \cap \mathcal{V}_{\mathcal{L}_c^{'}} = \emptyset, \mathcal{V}_{\mathcal{K}_c} \cap \mathcal{V}_{\mathcal{K}_c^{'}} = \emptyset, (c \neq c^{'}) \\ \left\{\mathcal{V}_{\mathcal{L}_c}, \mathcal{V}_{\mathcal{L}_c^{'}}\right\} \in L, \left\{\mathcal{V}_{\mathcal{K}_c}, \mathcal{V}_{\mathcal{K}_c^{'}}\right\} \in K. \tag{15}$$

*1) **User set formation**:* The K-means algorithm divides the K users into C clusters based on the high and low similarities within each cluster and among clusters. This can be achieved by minimizing the total distance among users within each cluster to its centroid. The cluster c is determined by a centroid calculated using the location of the users in the subset $\mathcal{V}_{\mathcal{K}_c}$ denoted by $\xi_c(I)$, where $I, i = \{0, \ldots, I\}$, is the total number of iterations. In this sense, the K users are defined as points in a 2-dimensional space as is shown in Fig. 2. Hence, the position of user k is defined by the tuple (x_k, y_k). Taking into consideration the number of clusters C, the initial centroids, i.e., $\xi_1(i), \xi_2(i), \ldots, \xi_C(i)$, correspond to the location of a random user. After that, the clustering formation is processed based on calculating the distance of each user from each centroid, i.e.,

$$\text{dist}(k, \xi_c(i)) = \sqrt{(x_k - x_{\xi_c(i)})^2 + (y_k - y_{\xi_c(i)})^2}, \tag{16}$$

where $\text{dist}(k, \xi_c(i))$ is the Euclidean distance and $\left(x_{\xi_c(i)}, y_{\xi_c(i)}\right)$ represents the coordinates of the cluster centroid $\xi_c(i)$ at the i-th iteration. Thus, user k is assigned to the clusters corresponding to the nearest centroid, i.e.,

$$c^* = \underset{c \in C}{\arg\min} \ \ \text{dist}(k, \xi_c(i)). \tag{17}$$

Notice that, if more than one centroid satisfies the condition (17) during a given iteration, user k is assigned randomly to one of them. Then, each cluster recalculates its centroid according to the coordinates of the newly included user as,

$$\xi_c(i+1) = \left(\frac{x_k + x_{\xi_c(i)}}{2}, \frac{y_k + y_{\xi_c(i)}}{2}\right). \tag{18}$$

After each iteration, the equations (16) and (17) are repeatedly checked until there is no change in the centroids of the clusters (18).

*2) **Optical AP Association**:* Aiming to guarantee the quality of the services provided and satisfying the user demands, we propose a novel optical AP association for the users belonging to each cluster based on average received power level. The sets of optical APs and users that compose the cluster c, which are denoted by $\mathcal{V}_{\mathcal{L}_c}$ and $\mathcal{V}_{\mathcal{K}_c}$, respectively, must be determined ensuring full connectivity within the cluster in order to maximize the DoF and the utilization of the transmission resources for BIA schemes. Therefore, a minimum threshold for the received power must be applied to avoid including useless optical APs. From a UC perspective, these optical APs sets update and change in a dynamic fashion as the users sets are formed as described above. The proposed optical APs association works as follows:

Each set of users $\mathcal{V}_{\mathcal{K}_c}$ is able to define its corresponding optical APs set $\mathcal{V}_{\mathcal{L}_c}$ based on local measurements only and independently of other users sets. Moreover, each user belonging to set $\mathcal{V}_{\mathcal{K}_c}$ sorts the optical APs according to their received power level. Thus, user k is associated with the optical APs that satisfy the condition

$$L_k^* = \arg\max \sum_{l \in L} \left(P_l^{[k,c]}\right), \ k \in \mathcal{V}_{\mathcal{K}_c}, \ l \in L, \tag{19}$$

where $P_l^{[k,c]}$ is the received power from optical AP l by user k belonging to set $\mathcal{V}_{\mathcal{K}_c}$. Notice that the received power level should not be lower than the minimum threshold power, i.e.,

$$P_l^{[k,c]} > P_{\min}^{[k,c]}, \tag{20}$$

where $P_{\min}^{[k,c]}$ is the minimum threshold power received by user k. Notice that each user receives the strongest signal power from the nearest optical AP. Thus, the optical APs that solve equation (19) are subject to the following constraint

$$l \in L \,/\, \text{dist}\left(l, \xi_c(I)\right) \leq d_{\text{th}}, \tag{21}$$

where $\text{dist}\left(l, \xi_c(I)\right)$ is the distance between optical AP l and the centroid of users set $\mathcal{V}_{\mathcal{K}_c}$ and d_{th} is the threshold distance between optical AP and the centroid of the cluster.

As a consequence, the combination of optical APs of each user is constrained by (20) and (21). It is worth mentioning that the users belonging to set $\mathcal{V}_{\mathcal{K}_c}$ are grouped based on the closest distance, and therefore, their combinations of optical APs resulting from equation (19) are overlapping with each other, forming the optical APs set $\mathcal{V}_{\mathcal{L}_c}$. Furthermore, after gradually constructing all the optical APs sets by the aforementioned rules, if a specific optical AP belongs to several optical APs sets, i.e., $l^* \in (\mathcal{V}_{\mathcal{L}_c} \cap \mathcal{V}_{\mathcal{L}_c^{'}})$, this optical AP selects the cluster with closest centroid, i.e.,

$$\mathcal{V}_{\mathcal{L}_c} = \left\{l^* \,/\, \arg\min \ \ \text{dist}\left(l^*, \xi_c(I)\right)\right\}. \tag{22}$$

Besides, if multiple centroids have the same distance to optical AP l^*, it is assigned randomly to one of them. As a result, the proposed scheme ends up with a unique optical APs set for each UC cluster.

In Fig. 8, the proposed UC design is applied, and then, the whole area of the VLC network is divided into three elastic clusters, i.e., $C = 3$. Moreover, the constructed UC clusters change over time to adapt to the updates of the VLC network topology, for example an optical AP might be turned on or off or the distribution of the users may vary. It is worth mentioning that our UC formation requires a pre-estimated number of

clusters in order to find the optimal solution. In Section VI, different values of C are tested.

B. DoF and achievable rates for UC-BIA

Assuming the implementation of BIA in each cluster, the proposed UC approach improves both the achievable DoF and user rates. For the toy example depicted in Fig. 7(c), the NC approach generates two clusters composed of two optical APs and two users each. Since BIA transmission is considered in each cluster, the NC approach achieves $\frac{4}{3}+\frac{4}{3}\approx 2.6$ DoF and each user suffers a noise enhancement because of removing the interference due to transmission to the other user in the same cluster. Moreover, the coherence time must be large enough to consider a supersymbol length comprising 3 time slots. On the other hand, the UC approach depicted in Fig. 7(d) generates three clusters; two of them with a single AP and a single user and one cluster with two optical APs and two users. Thus, the achievable DoF equals to $1+\frac{4}{3}+1\approx 3.3$ DoF, which outperforms the DoF achieved by the NC approach. Moreover, the users within the clusters composed of a single AP do not suffer any noise increase and the supersymbol length comprises a unique time slot. For the general case, the UC approach combined with BIA schemes reduces the constraints related to the required SNR and coherence time, which makes its implementation more suitable for VLC networks.

Each cluster c implements a BIA scheme independently of all other clusters. Moreover, the sets of optical APs and users that define cluster c do no overlap with other clusters (see (15)). Thus, considering $|\mathcal{V}_{\mathcal{L}_c}|=L_c$ denoting the number of optical APs and $|\mathcal{V}_{\mathcal{K}_c}|=K_c$ denoting the number of users within cluster c, the supersymbol comprises

$$\Gamma_{\mathrm{UC-BIA}}=(L_c-1)^{K_c}+K_c(L_c-1)^{K_c-1}, \tag{23}$$

time slots. As a consequence, $(L_c-1)^{K_c-1}$ alignment blocks are allocated to each user of cluster c and L_c DoF can be decoded over each alignment block. Therefore, the normalized sum-DoF achievable for the proposed UC-BIA is

$$\mathrm{DoF}_{\mathrm{UC-BIA}}=\sum_{c=1}^{C}\frac{L_cK_c}{L_c+K_c-1}. \tag{24}$$

The proposed UC approach minimizes the inter-cluster interference and, therefore, it can be treated as noise. Thus, the signal received by user k, $k\in\mathcal{V}_{\mathcal{K}_c}$, during its alignment block $\zeta,\zeta\zeta=\{1,\ldots,(L_c-1)^{K_c-1}\}$, after aligning and subtracting the interference can be written as

$$\mathbf{y}^{[k,c]}=\mathbf{H}_c^{[k,c]}\mathbf{u}_{\zeta}^{[k,c]}+\sum_{c'=1,c'\neq c}^{C}\sqrt{\alpha_{c'}^{[k,c]}}\mathbf{H}_{c'}^{[k,c']}\mathbf{u}_{\zeta}^{[k,c']}+\mathbf{z}^{[k,c]}, \tag{25}$$

where $\alpha_{c'}^{[k,c]}$ is the relative power from optical cluster c' received at user k in cluster c taking this cluster as reference, i.e., $\alpha_c^{[k,c]}=1$, denoting $\mathbf{h}_{c'}^{[k,c]}(m)\in\mathbb{R}^{L_{c'}\times 1}$ as the channel between the $L_{c'}$ optical APs that compose cluster c' and user k in cluster c at preset mode m, $\mathbf{H}_{c'}^{[k,c]}$ is defined as

$$\mathbf{H}_{c'}^{[k,c]}=\left[\mathbf{h}_{c'}^{[k,c]}(1)\quad\ldots\mathbf{h}_{c'}^{[k,c']}(L_c)\right]^T\in\mathbb{R}^{L_c\times L_{c'}}, \tag{26}$$

where $\mathbf{H}_c^{[k,c]}$ is the channel matrix for cluster c in similar fashion as (12) while $\mathbf{H}_{c'}^{[k,c]}$, $c'\neq c$, represents the interference received from neighbouring clusters. Finally, in (25), $\mathbf{z}^{[k,c]}$ represents the noise after interference subtraction, which is given by a covariance matrix as

$$\mathbf{R}_{\mathbf{z_p}}=\begin{bmatrix}K_c\mathbf{I}_{L_c-1} & \mathbf{0}\\ \mathbf{0} & 1\end{bmatrix}. \tag{27}$$

Thus, the achievable data rate of user k belonging to cluster c is given by

$$r^{[k,c]}=b^{[k,c]}\mathbb{E}\left[\log\det\left(\mathbf{I}_L+P_{str}\mathbf{H}_c^{[k,c]}{\mathbf{H}_c^{[k,c]}}^H\mathbf{R}_{\tilde{\mathbf{z}}}^{-1}\right)\right], \tag{28}$$

where $b^{[k,c]}=\frac{1}{L_c+K_c-1}$ is the ratio of the alignment blocks allocated to user k during the entire supersymbol and, since the inter-cluster interference is treated as noise,

$$\mathbf{R}_{\tilde{\mathbf{z}}}=\mathbf{R}_{\mathbf{z_p}}+P_{str}\sum_{c'=1,c'\neq c}^{C}\alpha_{c'}^{[k,c]}\mathbf{H}_{c'}^{[k,c]}{\mathbf{H}_{c'}^{[k,c]}}^H, \tag{29}$$

is the covariance matrix of the noise plus interference.

V. Resource Allocation in User Centric Cluster

In this section, we formulate an optimization problem for the resource allocation in order to satisfy the demands of the users taking into consideration the topology of the VLC network. In particular, the most computationally efficient method to find the resource allocation for each user is to simply implement a uniform resource allocation scheme. In this manner, users associated with an optical AP share its available resources uniformly. Notice that, the proposed UC approach guarantees full connectivity within each cluster. Therefore, the BIA scheme can be implemented into each cluster as a MISO BC, i.e., users belonging to set $\mathcal{V}_{\mathcal{K}_c}$ get resources from all the available optical APs of set $\mathcal{V}_{\mathcal{L}_c}$. As a consequence, we assume that the available resources of each optical AP l, $l\in\mathcal{V}_{\mathcal{L}_c}$, in terms of the fractional time denoted by $e^{[l,c]}$ are uniformly allocated among the users belonging to set $\mathcal{V}_{\mathcal{K}_c}$, i.e., uniformly among the alignment blocks $K_c(L_c-1)^{K_c-1}$ obtained by the implementation of the BIA scheme. Therefore, the resources allocated to each user belonging to set $\mathcal{V}_{\mathcal{K}_c}$ of cluster c are given by

$$e^{[k,c]}=\sum_{l\in\mathcal{V}_{\mathcal{L}_c}}\frac{e^{[l,c]}}{|\mathcal{V}_{\mathcal{K}_c}|},\ \forall l\in\mathcal{V}_{\mathcal{L}_c},\forall k\in\mathcal{V}_{\mathcal{K}_c},\forall c\in C. \tag{30}$$

Notice that, $e^{[k,c]}$ can be defined as a fractional variable corresponding to the time that cluster c devotes to communicate with user k. Despite the simplicity of the uniform resource allocation scheme, it might waste the network resources due to the fact that the users belonging to cluster c may not need to employ their resources fully. Therefore, the uniform resource allocation scheme may lead to reducing the overall resource utilization into the area of each UC cluster. In this work, we are aiming to solve this issue through formulating a resource allocation optimization problem that considers the demands of the users.

In the following, the optimization problem is formulated based on maximizing the aggregate utility-based resource

function taking into consideration the constructed UC clusters. Then, we propose a centralized algorithm to solve the optimization problem through an exhaustive search method and find the optimal resource allocation in the whole VLC area. After that, a distributed algorithm is proposed in order to reduce the complexity while providing a near optimal alternative to the centralized algorithm through giving both the users and the optical APs active roles to solve the optimization problem.

A. Problem formulation and centralized algorithm

The concept of utility function can be adopted to model the resource allocation problem for a VLC network serving multiple users. The resources allocated from optical AP l, $l \in \mathcal{V}_{\mathcal{L}_c}$, to user k, $k \in \mathcal{V}_{\mathcal{K}_c}$, are denoted[4] by $e^{[k,l,c]}$. Thus, the resources allocated to each user belonging to $\mathcal{V}_{\mathcal{K}_c}$ can be determined as

$$e^{[k,c]} = \sum_{l \in \mathcal{V}_{\mathcal{L}_c}} e^{[k,l,c]}, \ \forall l \in \mathcal{V}_{\mathcal{L}_c}, \forall k \in \mathcal{V}_{\mathcal{K}_c}, \forall c \in C. \quad (31)$$

The overall rate of user k, which is derived in (28), can be expressed as

$$R^{[k,c]} = e^{[k,c]} \ r^{[k,c]}. \quad (32)$$

Our objective function aims to allocate the network resources based on the demands of users in order to guarantee the maximization of their utilization. We consider that the resources allocated to each user belonging to set $\mathcal{V}_{\mathcal{K}_c}$ from their corresponding optical APs into set $\mathcal{V}_{\mathcal{L}_c}$ must be in the range $\left[e_{\min}^{[k,c]}, e_{\max}^{[k,c]}\right]$. The value $e_{\min}^{[k,c]}$ corresponds to the overall minimum resources required by user k to achieve a minimum data rate. On the other hand, the value $e_{\max}^{[k,c]}$ is defined as the overall maximum resources required by user k to further improve the achievable user rate. According to the load of cluster c, the minimum or maximum required resources are allocated to user k. For example, if there are sufficient resources into cluster c, user k increases towards the maximum value $e_{\max}^{[k,c]}$, otherwise, the allocated resources decrease to the minimum value $e_{\min}^{[k,c]}$.

In order to find the overall resource allocated to each user, an optimization problem is formulated based on maximizing the aggregate utility function of the resources allocated to the users belonging to each cluster c [26], [37]. That is,

$$\begin{aligned} \max_{e} \quad & U\left(e^{[k]}\right) = \sum_{c \in C} \sum_{l \in \mathcal{V}_{\mathcal{L}_c}} \sum_{k \in \mathcal{V}_{\mathcal{K}_c}} \log\left(1 + \eta_k \ e^{[k,l,c]}\right) \\ \text{s.t.} \quad & \sum_{k \in \mathcal{V}_{\mathcal{K}_c}} e^{[k,l,c]} \leq \alpha_l, \ \forall l \in \mathcal{V}_{\mathcal{L}_c}, \ \forall c \in C \\ & e_{\min}^{[k,c]} \leq e^{[k,c]} \ b^{[k,c]} \leq e_{\max}^{[k,c]}, \ \forall k \in \mathcal{V}_{\mathcal{K}_c}, \ \forall c \in C, \end{aligned} \quad (33)$$

where $U(\cdot)$ is a monotonically increasing, strictly concave and continuously differentiable function, which achieves proportional fairness among users, e.g., considering a logarithmic function $U(\cdot) = \log(\cdot)$ [38], $\eta_k > 0$ is the scalability to flow $e^{[l,k,c]}$ [37], α_l is the capacity constraint of optical AP l, $l \in \mathcal{V}_{\mathcal{L}_c}$, and $b^{[k,c]}$ is the ratio of alignment blocks allocated for user k, which is defined in (28). It is worth mentioning that the objective function is considered in the form of $\log\left(1 + \eta_k \ e^{[k,l,c]}\right)$ in order to avoid the case of having $U(\cdot) = -\infty$ if $e^{[k,l,c]} = 0$. The first constraint satisfies the requirement that the resources allocated to each user belonging to set $\mathcal{V}_{\mathcal{K}_c}$ from each optical AP l into set $\mathcal{V}_{\mathcal{L}_c}$ are equal or less than the capacity limitation of that optical AP, while the second constraint guarantees that the total resources allocated for each user belonging to cluster c are within the range of its needs. This optimization problem can be solved through an exhaustive search method. This method is denoted as a centralized algorithm from now on, and it requires a central manager to control the network resource allocation, in addition to some network information and coordination among the optical APs. As a consequence, the centralized algorithm requires high computational complexity to find the optimal solution even for a modest size of the VLC network.

In the following, we propose a distributed algorithm in which the problem in (33) can be divided into C smaller problems. Moreover, the dual decomposition via Lagrangian multiplier method is considered to solve the optimization problem within each UC cluster, i.e., the resource allocation problem of each UC cluster is decoupled into two subproblems, which can be solved jointly by an iterative algorithm or separately at the users side and the optical APs side, respectively.

B. Distributed resource allocation

A full dual decomposition method is proposed whereby using the Lagrangian multiplier [26], [39], [40] can be adopted to solve the optimization problem in (33). First, the problem in (33) can be rewritten for a given UC cluster as

$$\begin{aligned} \max_{e} \quad & \sum_{l \in \mathcal{V}_{\mathcal{L}_c}} \sum_{k \in \mathcal{V}_{\mathcal{K}_c}} \log\left(1 + \eta_k \ e^{[k,l,c]}\right) \\ \text{s.t.} \quad & \sum_{k \in \mathcal{V}_{\mathcal{K}_c}} e^{[k,l,c]} \leq \alpha_l, \ \forall l \in \mathcal{V}_{\mathcal{L}_c}, \ \forall c \in C \\ & \sum_{l \in \mathcal{V}_{\mathcal{L}_c}} e^{[k,l,c]} \ b^{[k,c]} \geq e_{\min}^{[k,c]}, \ \forall k \in \mathcal{V}_{\mathcal{K}_c}, \forall c \in C \\ & \sum_{l \in \mathcal{V}_{\mathcal{L}_c}} e^{[k,l,c]} \ b^{[k,c]} \leq e_{\max}^{[k,c]}, \ \forall k \in \mathcal{V}_{\mathcal{K}_c}, \forall c \in C. \end{aligned} \quad (34)$$

Then, the Lagrangian function for (34) is given by (35), where ε_l, λ_k and ν_k are the Lagrange multipliers associated with the first, second and last constraints in (34), respectively. The dual function can be expressed as the maximum value of the Lagrangian function, i.e.,

$$\mathcal{G}(\varepsilon, \lambda, \nu) = \max_{e} f(e, \varepsilon_l, \lambda_k, \nu_k). \quad (36)$$

As a consequence, the optimum value of $e^{[k,l,c]}$ can be obtained by solving the following dual problem

$$\min_{\varepsilon, \lambda, \nu} \mathcal{G}(\varepsilon, \lambda, \nu). \quad (37)$$

[4]We consider that each optical AP l, $l \in \mathcal{V}_{\mathcal{L}_c}$, gives the highest priority for allocating its resources to user k, $k \in \mathcal{V}_{\mathcal{K}_c}$, that satisfies $k \in \mathcal{V}_{\mathcal{K}_c}$ / $\operatorname{argmin} \operatorname{dist}(k, l)$.

$$f\left(e,\varepsilon_l,\lambda_k,\nu_k\right)=\sum_{l\in\mathcal{V}_{\mathcal{L}_c}}\sum_{k\in\mathcal{V}_{\mathcal{K}_c}}\log\left(1+\eta_k\ e^{[k,l,c]}\right)+\underbrace{\sum_{l\in\mathcal{V}_{\mathcal{L}_c}}\varepsilon_l\left(\alpha_l-\sum_{k\in\mathcal{V}_{\mathcal{K}_c}}e^{[k,l,c]}\right)}_{\text{constraint 1 in (34)}}$$
$$+\underbrace{\sum_{k\in\mathcal{V}_{\mathcal{K}_c}}\lambda_k\left(b^{[k,c]}\sum_{l\in\mathcal{V}_{\mathcal{L}_c}}e^{[k,l,c]}-e^{[k,c]}_{\min}\right)}_{\text{constraint 2 in (34)}}+\underbrace{\sum_{k\in\mathcal{V}_{\mathcal{K}_c}}\nu_k\left(e^{[k,c]}_{\max}-b^{[k,c]}\sum_{l\in\mathcal{V}_{\mathcal{L}_c}}e^{[k,l,c]}\right)}_{\text{constraint 3 in (34)}} \tag{35}$$

Interestingly, the problem in (34) is a convex optimization problem where the constraints are all linear equalities. Therefore, the optimal value can be equivalently found by solving the dual problem of (37) [41]. In this sense, we propose a distributed algorithm via Lagrangian decomposition to solve the problem in (37). Notice that, the dual function in (36) can be simplified to

$$\mathcal{G}(\varepsilon,\lambda,\nu)=\sum_{l\in\mathcal{V}_{\mathcal{L}_c}}\max_{e}\left\{\sum_{k\in\mathcal{V}_{\mathcal{K}_c}}\log\left(1+\eta_k\ e^{[k,l,c]}\right)-\varepsilon_l\sum_{k\in\mathcal{V}_{\mathcal{K}_c}}e^{[k,l,c]}-\sum_{k\in\mathcal{V}_{\mathcal{K}_c}}\left(\nu_k-\lambda_k\right)\ e^{[k,l,c]}\right\}. \tag{38}$$

Algorithm 1 Distributed resource Allocation

1: **Input**: $e^{[k,c]}_{\min}$ and $e^{[k,c]}_{\max}$ for each user $k\in\mathcal{V}_{\mathcal{K}_c}$, α_l for each AP $l\in\mathcal{V}_{\mathcal{L}_c}$;
2: **Initialisation**: $i=0$, ε_l for each AP $l\in\mathcal{V}_{\mathcal{L}_c}$, λ_k and ν_k for each user $k\in\mathcal{V}_{\mathcal{K}_c}$, step size $\Omega_j(i)>0$, $j\in\{\varepsilon,\lambda,\nu\}$;
3: **for** each $c\in C$ **do**;
4: **for** each AP $l\in\mathcal{V}_{\mathcal{L}_c}$ **do**;
5: Solve (39);
6: Update ε_l according to (47) ;
7: **end for**
8: **for** each user $k\in\mathcal{V}_{\mathcal{K}_c}$ **do**;
9: Update λ_k and ν_k according to (48) and (49);
10: Update $(\nu_k-\lambda_k)$;
11: **end for**
12: $i=i+1$;
13: Update $\Omega_j(i+1)$, $j\in\{\varepsilon,\lambda,\nu\}$, according to (50);
14: **end for**

The distributed algorithm works as follows. First, according to (38), each optical AP l, $l\in\mathcal{V}_{\mathcal{L}_c}$, can solve its own optimization problem independently from the other optical APs into set $\mathcal{V}_{\mathcal{L}_c}$ with the aim of finding the optimum $e^{*[k,l,c]}$ [26]. Thus, the optimization problem of optical AP l into cluster c can be expressed as

$$e^{*[k,l,c]}=\arg\max_{e}g(e), \tag{39}$$

where

$$g(e)=\sum_{k\in\mathcal{V}_{\mathcal{K}_c}}\log\left(1+\eta_k\ e^{[k,l,c]}\right)-\varepsilon_l\sum_{k\in\mathcal{V}_{\mathcal{K}_c}}e^{[k,l,c]}-\sum_{k\in\mathcal{V}_{\mathcal{K}_c}}\left(\nu_k-\lambda_k\right)\ e^{[k,l,c]}. \tag{40}$$

It can be seen that the problem in (39) is a concave problem with respect to the variable $e^{[k,l,c]}$. Therefore, the optimum value $e^{*[k,l,c]}$ can be calculated by taking the partial derivative of (40) with respect to $e^{[k,l,c]}$ as

$$\frac{\partial g(e)}{\partial e}=\left(\frac{\partial\sum_{k\in\mathcal{V}_{\mathcal{K}_c}}\log\left(1+\eta_k\ e^{[k,l,c]}\right)}{\partial e}\right)-\varepsilon_l-(\nu_k-\lambda_k). \tag{41}$$

As a consequence, $\frac{\partial g(e)}{\partial e}$ is a monotonically decreasing function with respect to the resource allocated $e^{[k,l,c]}$ by optical AP l for all the users belonging to cluster c. Given this point, if the partial derivative $\frac{\partial g(e)}{\partial e}|_{e^{[k,l,c]}=0}\leq 0$, the optimum value $e^{*[k,l,c]}$ equals zero. Furthermore, if the partial derivative $\frac{\partial g(e)}{\partial e}|_{e^{[k,l,c]}=1}\geq 0$, the optimum value $e^{*[k,l,c]}$ equals one. On the other hand, the optimum value $e^{*[k,l,c]}$ can be calculated by solving the following equation for each optical AP l into cluster c

$$\left(\frac{\partial\sum_{k\in\mathcal{V}_{\mathcal{K}_c}}\log\left(1+\eta_k\ e^{[k,l,c]}\right)}{\partial e}\right)=\varepsilon_l+(\nu_k-\lambda_k), \tag{42}$$

where ε_l, λ_k and ν_k correspond to fixed values. Therefore, the optimum resource allocation is given as

$$e^{*[k,l,c]}=\frac{\eta_k}{\varepsilon_l+(\nu_k-\lambda_k)}-1/\eta_k. \tag{43}$$

As a results, the optimum value $e^{*[k,l,c]}$, where $\forall l\in\mathcal{V}_{\mathcal{L}_c}$, ,$\forall k\in\mathcal{V}_{\mathcal{K}_c}$ and $\forall c\in C$, is equal to

$$e^{*[k,l,c]}=\begin{cases}0, & \frac{\partial g\left(e\right)}{\partial e}|_{e^{[k,l,c]}=0}\leq 0\\ 1, & \frac{\partial g\left(e\right)}{\partial e}|_{e^{[k,l,c]}=1}\geq 0\\ \frac{\eta_k}{\varepsilon_l+(\nu_k-\lambda_k)}-1/\eta_k, & \text{otherwise.}\end{cases} \tag{44}$$

Secondly, the dual problem of (37), taking into account the

optimum value $e^{*[k,l,c]}$ derived from the first step, can be modified according to the following equation to calculate the optimum values of the multipliers ε_l, λ_k and ν_k

$$\min_{\varepsilon,\lambda,\nu}\{f(g(e*),\varepsilon_l,\lambda_k,\nu_k)\}, \tag{45}$$

where

$$\begin{aligned} f(g(e*),\varepsilon_l,\lambda_k,\nu_k) &= \sum_{l\in\mathcal{V}_{\mathcal{L}_c}} \varepsilon_l \left(\alpha_l - \sum_{k\in\mathcal{V}_{\mathcal{K}_c}} e^{*[k,l,c]}\right) \\ &+ \sum_{k\in\mathcal{V}_{\mathcal{K}_c}} \lambda_k \left(b^{[k,c]} \sum_{l\in\mathcal{V}_{\mathcal{L}_c}} e^{*[k,l,c]} - e^{[k,c]}_{\min}\right) \\ &+ \sum_{k\in\mathcal{V}_{\mathcal{K}_c}} \nu_k \left(e^{[k,c]}_{\max} - b^{[k,c]} \sum_{l\in\mathcal{V}_{\mathcal{L}_c}} e^{*[k,l,c]}\right). \end{aligned} \tag{46}$$

It can be seen that the objective function in (45) is concave and differentiable, and therefore, the gradient projection method can be applied to solve it. As a result, the values for ε_l, λ_k and ν_k can be updated according to

$$\varepsilon_l(i+1) = \left[\varepsilon_l(i) - \Omega_\varepsilon(i)\left(\alpha_l - \sum_{k\in\mathcal{V}_{\mathcal{K}_c}} e^{*[k,l,c]}\right)\right]^+, \tag{47}$$

$$\lambda_k(i{+}1) = \left[\lambda_k(i) - \Omega_\lambda(i)\left(\sum_{l=1}^{|\mathcal{V}_{\mathcal{L}_c}|} e^{*[k,l,c]}\ b^{[k,c]} - e^{[k,c]}_{\min}\right)\right]^+, \tag{48}$$

$$\nu_k(i{+}1) = \left[\nu_k(i) - \Omega_\nu(i)\left(e^{[k,c]}_{\max} - \sum_{l=1}^{|\mathcal{V}_{\mathcal{L}_c}|} e^{*[k,l,c]}\ b^{[k,c]}\right)\right]^+, \tag{49}$$

respectively, where $i-$th denotes the iteration of the gradient algorithm, $[.]^+$ is a projection on the positive orthant to account for considering the fact that we have $\varepsilon_l, \lambda_k, \nu_k \geq 0$. Furthermore, $\Omega_j(i)$, $j \in \{\varepsilon, \lambda, \nu\}$, is the step size at a given $i-$th iteration that is taken in the direction of the negative gradient for the multipliers ε_l, λ_k and ν_k.

Based on the above discussion, the distributed algorithm can be solved iteratively. In this sense, each optical APs into set $\mathcal{V}_{\mathcal{L}_c}$ calculates the optimum resource allocation through solving the optimization problem defined in (39), which has the optimum solution of (44) considering different cases. After that, the dual problem defined in (45) can be solved over a number of iterations in order to obtain the optimum solution and set the multipliers ε_l, λ_k and ν_k. As a results, the sub problem in (39) can be coordinated.

Finally, the dual problem can be solved separately on the users side and the optical APs side, respectively. In this sense, the multipliers ε_l, λ_k and ν_k work as messages between the users set $\mathcal{V}_{\mathcal{K}_c}$ and the optical APs set $\mathcal{V}_{\mathcal{L}_c}$ that compose cluster c. The multiplier ε_l can be interpreted as the price of optical AP l, $l \in \mathcal{V}_{\mathcal{L}_c}$, and hence, it is determined according to the capacity limitation α_l. By simply interpreting the traffic load on optical AP l into cluster c, i.e., $(\sum_{k\in\mathcal{V}_{\mathcal{K}_c}} e^{[k,l,c]})$, as the traffic demand, the multiplier ε_l works as a bridge between the traffic demand and the capacity limitation of optical AP l.

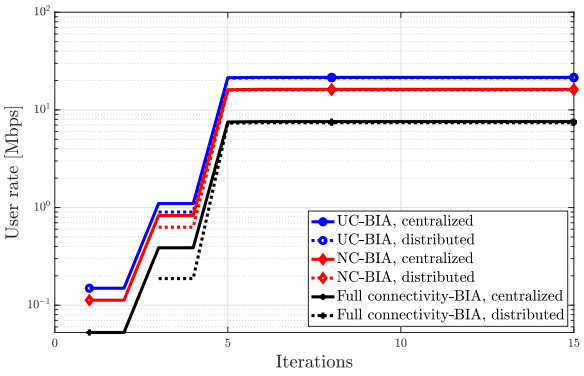

Fig. 9. The optimality of the distributed algorithm in comparison with the centralized algorithm. Different optical cluster formations are considered based on BIA schemes. $C = 3$ clusters are assumed for UC and NC approaches.

For example, if the traffic demand of optical AP l, $l \in \mathcal{V}_{\mathcal{L}_c}$, exceeds its capacity limitation, the price ε_l goes up in order to denote that it is expensive to use this link, otherwise, the price ε_l decreases to state the low cost of using this link. On the other hand, the multipliers λ_k and ν_k are used by each user belonging to the users set $\mathcal{V}_{\mathcal{K}_c}$ of cluster c to ensure that the resources allocated for each user fall within the required range of the resources. As a results, each optical AP in cluster c starts with an initial feasible value for its price, and then, updates that price based on its own traffic demand and capacity limitation. Similarly, each user belonging to cluster c starts with an initial feasible value for its coordination parameters, and then, updates and broadcasts the difference $(\nu_k - \lambda_k)$ to all the optical APs of cluster c in order to coordinate the resource allocation. As a consequence, the total amount of the resources allocated to each user satisfies its demand. The distributed resource allocation is summarized in **Algorithm 1**.

C. Optimality and convergence

After iteratively performing the process above, the distributed algorithm is guaranteed to converge and provide a solution significantly close to the optimal. In Fig. 9, the achievable user rate is depicted over a dozen of iterations and based on the simulation parameters discussed in Section VI. It can be seen that the proposed algorithm is capable of converging to the optimal solution provided by the centralized algorithm with lower complexity. This near optimal solution can be achieved by updating the step size parameters according to the following procedure.

Focussing on the step size Ω_ε, it is updated by

$$\Omega_\varepsilon(i) = \left(\frac{\mathcal{G}(\varepsilon(i)) - \mathcal{G}(i)}{(\Lambda_\varepsilon(i))^2}\right)\kappa_1(i), \tag{50}$$

where $\Lambda_\varepsilon(i) = \|\mathcal{G}(\varepsilon(i))\|$, and $0 \leq \kappa_1(i) \geq 2$ is some scalar [42], [43]. Moreover, $\mathcal{G}(i)$ is the optimal value of the optimization problem in (36). It is updated as in the following

$$\mathcal{G}(i) = \min_{0\leq\iota\leq i} \mathcal{G}(\varepsilon(\iota)) - \delta_\varepsilon(i), \tag{51}$$

where $\delta_\varepsilon(i)$ can be defined as a value that guarantees that the step size Ω_ε is not equal to zero at a given iteration, i.e.,

$\Omega_\varepsilon \neq 0$. This condition can be satisfied by either increasing $\delta_\varepsilon(i)$ or by keeping it at the same value if the target value $\mathcal{G}(i)$, which is smaller by $\delta_\varepsilon(i)$ than the best value (see 51), is achieved. On the other hand, if the target value is not obtained at a given iteration, $\delta_\varepsilon(i)$ is decreased towards a threshold value of δ_ε. As a consequence, $\delta_\varepsilon(i)$ is given by

$$\delta_\varepsilon(i) = \rho\ \delta_\varepsilon(i-1),\ \rho \geq 1, \tag{52}$$

in the case that $\mathcal{G}(\varepsilon(i)) \leq \mathcal{G}(\varepsilon(i-1))$. Otherwise, it is given by

$$\delta_\varepsilon(i) = \max\{\omega\ \delta_\varepsilon(i-1), \delta_\varepsilon\},\ \omega > 1, \tag{53}$$

where ρ and ω are fixed positive numbers [43]. According to the procedure described above for updating the step size Ω_ε, if the optimal value of $\mathcal{G}$, which is denoted as $\mathcal{G}^*$, where $\mathcal{G}^* > -\infty$, is obtained, the following condition is satisfied

$$\inf_i \mathcal{G}(\varepsilon(i)) \leq \mathcal{G}^* + \delta_\varepsilon. \tag{54}$$

Notice that, the derivative of $\mathcal{G}(\varepsilon)$ in (36) is

$$\frac{\partial \mathcal{G}(\varepsilon)}{\partial \varepsilon} = \alpha_l - \sum_{k \in \mathcal{V}_{\mathcal{K}_c}} e^{[k,l,c]}, \tag{55}$$

where α_l and $\sum_{k \in \mathcal{V}_{\mathcal{K}_c}} e^{[k,l,c]}$ are bounded. Therefore, the subgradient of the dual objective function $\partial \mathcal{G}(\varepsilon)$ is also bounded,

$$\sup_t \{\Lambda_\varepsilon(i)\} \leq \kappa_2, \tag{56}$$

where κ_2 is some scalar. The same procedure is applied for updating the step size Ω_λ and Ω_ν values. Notice that, the derivatives of $\mathcal{G}(\lambda)$ and $\mathcal{G}(\nu)$ in (36) are given by

$$\frac{\partial \mathcal{G}(\lambda)}{\partial \lambda} = \sum_{l \in \mathcal{V}_{\mathcal{L}_c}} e^{[k,l,c]}\ b^{[k,c]} - e^{[k,c]}_{\min}, \tag{57}$$

and

$$\frac{\partial \mathcal{G}(\nu)}{\partial \nu} = e^{[k,c]}_{\max} - \sum_{l \in \mathcal{V}_{\mathcal{L}_c}} e^{[k,l,c]}\ b^{[k,c]}, \tag{58}$$

respectively. Referring to equation (57), $\sum_{l \in \mathcal{V}_{\mathcal{L}_c}} e^{[k,l,c]}\ b^{[k,c]}$ and $e^{[k,c]}_{\min}$ are bounded, and therefore, the subgradient of the dual objective function, $\partial \mathcal{G}(\lambda)$, is bounded,

$$\sup_t \{\Lambda_\lambda(i)\} \leq \kappa_3, \tag{59}$$

where κ_3 is some scalar. Similarly, in equation (58), $e^{[k,c]}_{\max}$ and $\sum_{l \in \mathcal{V}_{\mathcal{L}_c}} e^{[k,l,c]}\ b^{[k,c]}$ are bounded, and hence, the subgradient of the dual objective function $\partial \mathcal{G}(\nu)$ is bounded,

$$\sup_t \{\Lambda_\nu(i)\} \leq \kappa_4, \tag{60}$$

where κ_4 is some scalar.

The distributed algorithm satisfies the conditions required in [43] to provide a near optimal solution with low cost in terms of complexity. Thus, denoting the algorithm runtime complexity as Θ, the complexity of the distributed algorithm is equal to $\Theta\left(|\mathcal{V}_{\mathcal{L}_c}| \times |\mathcal{V}_{\mathcal{K}_c}|\right)$ at each iteration, while the complexity of the centralized algorithm is equal to $\Theta\left(\sum_{c=1}^{C} (|\mathcal{V}_{\mathcal{L}_c}|)^{|\mathcal{V}_{\mathcal{K}_c}|}\right)$, increasing exponentially with the network size. In terms of information exchanged, for the distributed algorithm, each optical AP and user into cluster c broadcast the price ε_l and the difference $(\nu_k - \lambda_k)$, respectively, which are relatively small real numbers. Hence, the amount of information exchanged at each iteration equals to $i \times (|\mathcal{V}_{\mathcal{L}_c}| + |\mathcal{V}_{\mathcal{K}_c}|)$. For the centralized algorithm, the complexity is proportional to $\sum_{c=1}^{C} (|\mathcal{V}_{\mathcal{L}_c}| \times |\mathcal{V}_{\mathcal{K}_c}|)$. From now on, we consider the distributed resource allocation algorithm since it provides results close to the optimal with lower complexity.

TABLE II
SIMULATION PARAMETERS

VLC parameter	Value
Bandwidth for each optical AP	20 MHz
Physical area of the photodiode	15 mm^2
Transmitter semi-angle	45 deg
Receiver FOV	70 deg
Detector responsivity	0.53 A/W
Gain of optical filter	1.0
Noise power spectral density	10^{-22}A^2/Hz

VI. PERFORMANCE EVALUATION

We now present the simulation results in which the performance of the proposed UC-BIA scheme is compared with other BIA schemes and also with TPC schemes such as ZF precoding and MRC detection. An indoor environment comprising a uniform distribution of 4×4 optical APs deployed on the ceiling of a $15\text{m} \times 15\text{m} \times 3\text{m}$ room is considered. The users are randomly distributed over a plane 2.15 m away from the ceiling. If it is not specified, the number of users is equal to $K = 20$, the maximum transmitted optical power of each optical LED is 10 dBW, and $C = 3$ clusters are considered. Each user is equipped with a reconfigurable photodetector able to switch among at least $M = 16$ preset modes following an hemispherical arrangement. All other simulation parameters are listed in **Table 1**.

The achievable user rate as the number of clusters increases is analyzed in Fig. 10. It can be seen that the user rate increases as the number of clusters grows until some point. Specifically, the user rate decreases for a value around 6 clusters for the considered scenario and for all the analyzed schemes. Moreover, the optimal value is between 4 and 6 user clusters, i.e., the user-rate is almost the same for these values. Notice that the number of clusters has a direct impact on the inter-cluster interference, and therefore, on the user rate. Furthermore, both UC approaches based on uniform and non-uniform resource allocation outperform the user rate achieved by NC clustering. The proposed resource allocation improves the overall user rate in comparison with uniform resource allocation.

In Fig. 11, the user rate achieved by the proposed non-uniform resource allocation is analyzed for distinct numbers of users, $K = \{10, 20, 30, 40\}$. It is shown that the non-uniform scheme achieves higher user rate in comparison with uniform resource allocation in all the considered scenarios. It can be seen that the user rate decreases as the number of

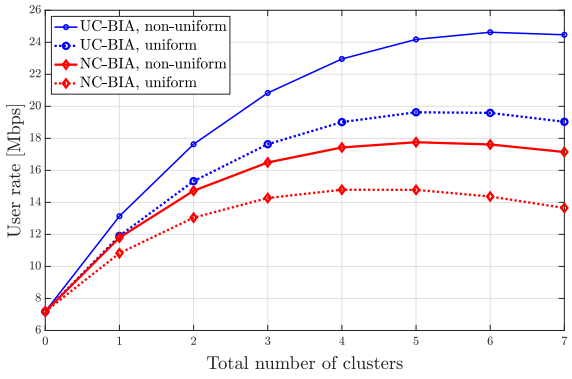

Fig. 10. Average user rate for the proposed schemes based on UC and NC approaches versus the number of clusters.

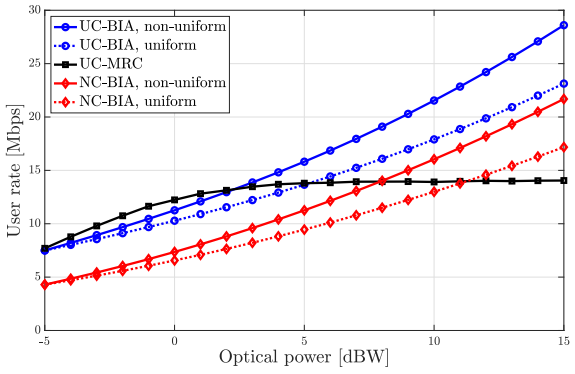

Fig. 12. Average user rate for the proposed schemes based on UC and NC approaches versus the transmitted optical power and in comparison with MRC.

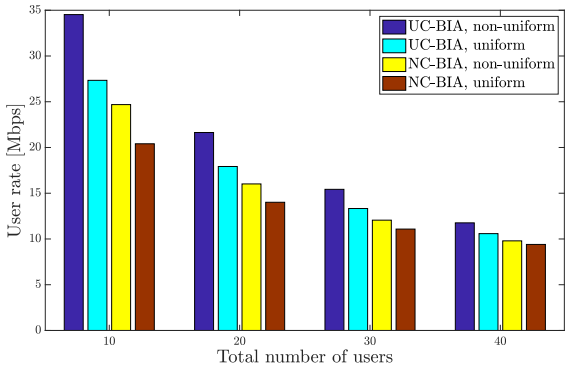

Fig. 11. Average user rate for the proposed schemes based on UC and NC approaches versus different number of users.

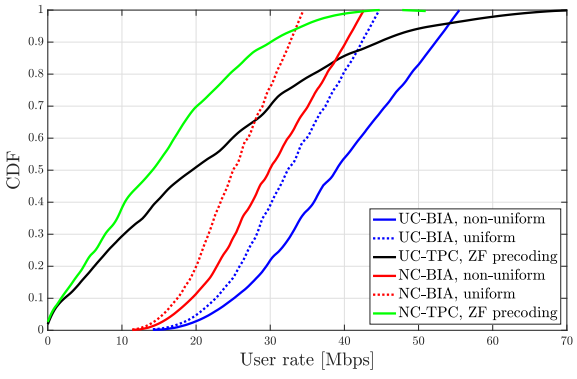

Fig. 13. CDF of the user rate for the non-uniform and uniform resource allocation schemes in comparison with TPC ZF precoding.

users increases due to the fact that less resources are available per user. Moreover, it is shown that the UC approach results are more suitable for VLC networks in comparison with NC clustering as the number of users increases. Notice that, in addition to the features of overcoming the limitations of BIA schemes such as the length of the supersymbol and the noise enhancement, the UC approach minimizes the ICI due to the elastic shapes of the formed clusters, which vary over time with the network topology updates.

The achievable user rate achieved by the proposed scheme in comparison with NC-BIA and MRC as the transmitted optical power increases is shown in Fig. 12. First, it is shown that the proposed non uniform resource allocation outperforms the uniform approach since each user obtains the required resources avoiding resource wastage. In comparison with a transmission scheme such as MRC, the user rate achieved by UC-BIA increases with the optical power, i.e., it works in the DoF regime. In contrast, the user-rate achieved by MRC remains constant beyond an optical power above 5 dBW. That is, increasing the optical power also involves increasing the interference above this point. Furthermore, as expected, it can be seen that the UC-BIA schemes, independently of the resource allocation scheme, achieve greater user rate than the NC-BIA schemes.

In Fig. 13, the cumulative distribution function (CDF) of the user-rate achieved by NC-BIA, UC-BIA and ZF precoding is depicted assuming both uniform and non-uniform resource allocation. It can be seen that non-uniform resource allocation provides a user-rate above 22 Mbps and 30 Mbps at the 20^{th} percentile for NC-BIA and UC-BIA, respectively. However, the user-rate is penalized considerably for the same transmission schemes is the resources are uniformly distributed. Specifically, at the 50^{th} percentile, uniform resource allocation involves a penalty of about 17% in comparison with the user rate achieved by non-uniform resource allocation. Furthermore, the performance of TPC schemes such as ZF precoding is subject to the correlation among the channel responses of the users. As a consequence, user rates below 10 Mbps are achieved at the 30^{th} percentile for both NC and UC clustering. In general, it can be seen that UC-BIA results are suitable for VLC networks while non-uniform resource allocation improves the overall user rate.

To conclude the analysis of the proposed schemes, the BER of binary pulse amplitude modulation (2-PAM) transmission achieved by NC-BIA and UC-BIA for uniform and non-uniform resource allocation is shown in Fig. 14. For the NC approach the BER is above 10^{-3} in the entire optical power range considered. Moreover, it can be seen that non-uniform resource allocation slightly improves the BER. In this sense, the management of the inter-cluster interference, i.e., the ICI among constructed optical cells, carried out by the UC approach allow us to improve the BER considerably.

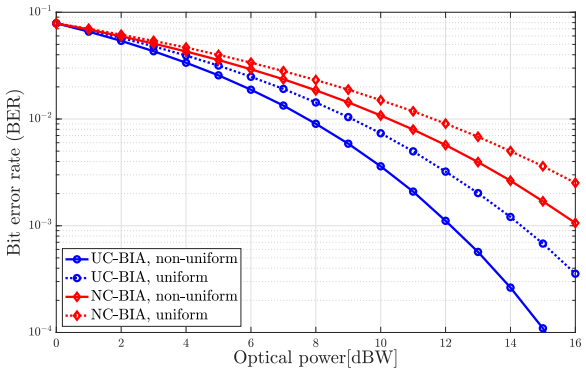

Fig. 14. BER for 2-PAM Modulation. No channel coding.

Specifically, a BER below 10^{-3} is achieved for an optical power greater than 13 dBW and 15 dBW for the non-uniform and uniform resource allocation schemes, respectively.

VII. Conclusions

In this work, we have approached the problem of resource allocation in VLC networks based on BIA schemes. We first propose a UC approach comprising two steps; *i)* several groups of users are formed based on the K-means algorithm, *ii)* the set of optical APs for each group of users is determined in order to guarantee full connectivity between all the users and the optical APs of each UC cluster. Based on this UC clustering, the implementation of BIA is considered in each cluster. With these clusters, the problem of resource allocation is formulated taking into consideration the network topology of the VLC network. Both centralized and distributed algorithms are proposed to solve the resource allocation problem. The centralized algorithm provides an optimal solution through exhaustive search with high complexity, while the distributed algorithm provides a near optimal solution to the centralized algorithm with much lower complexity. It is shown that the proposed algorithms provide higher user rates than traditional approaches based on NC and than other transmission schemes such as TPC and MRC. In addition, the BER achieved for BIA schemes applied to VLC networks is considerably improved by introducing the concepts of UC clustering and non-uniform resource allocation.

References

[1] H. Li, X. Chen, J. Guo, and H. Chen, "A 550 Mbit/s real-time visible light communication system based on phosphorescent white light LED for practical high-speed low-complexity application," *Opt. Express*, vol. 22, no. 22, pp. 27 203–27 213, Nov 2014.

[2] C. Wang, F. Haider, X. Gao, X. You, Y. Yang, D. Yuan, H. M. Aggoune, H. Haas, S. Fletcher, and E. Hepsaydir, "Cellular architecture and key technologies for 5G wireless communication networks," *IEEE Communications Magazine*, vol. 52, no. 2, pp. 122–130, February 2014.

[3] H. Elgala, R. Mesleh, and H. Haas, "Indoor optical wireless communication: potential and state-of-the-art," *IEEE Communications Magazine*, vol. 49, no. 9, pp. 56–62, Sep. 2011.

[4] C. Chen, D. Tsonev, and H. Haas, "Joint transmission in indoor visible light communication downlink cellular networks," in *2013 IEEE Globecom Workshops (GC Wkshps)*, Dec 2013, pp. 1127–1132.

[5] C. Chen, N. Serafimovski, and H. Haas, "Fractional frequency reuse in optical wireless cellular networks," in *2013 IEEE 24th Annual International Symposium on Personal, Indoor, and Mobile Radio Communications (PIMRC)*, Sep. 2013, pp. 3594–3598.

[6] X. Li, R. Zhang, and L. Hanzo, "Cooperative load balancing in hybrid visible light communications and WiFi," *IEEE Transactions on Communications*, vol. 63, no. 4, pp. 1319–1329, April 2015.

[7] X. Li, R. Zhang, J. Wang, and L. Hanzo, "Cell-centric and user-centric multi-user scheduling in visible light communication aided networks," in *2015 IEEE International Conference on Communications (ICC)*, June 2015, pp. 5120–5125.

[8] A. Adnan-Qidan, M. Morales-Cespedes, and A. Garcia-Armada, "User-centric blind interference alignment design for visible light communications," *IEEE Access*, vol. 7, pp. 21 220–21 234, 2019.

[9] ——, "Load balancing in hybrid VLC and RF networks based on blind interference alignment," *IEEE Access*, vol. 8, pp. 72 512–72 527, 2020.

[10] A. Adnan-Quidan, M. Morales-Cespedes, and A. Garcia-Armada, "Aligning the light based on the network topology for visible light communications," in *2018 IEEE International Conference on Communications Workshops (ICC Workshops)*, 2018, pp. 1–6.

[11] X. Li, F. Jin, R. Zhang, J. Wang, Z. Xu, and L. Hanzo, "Users first: User-centric cluster formation for interference-mitigation in visible-light networks," *IEEE Transactions on Wireless Communications*, vol. 15, no. 1, pp. 39–53, Jan 2016.

[12] A. Adnan-Qidan, M. Morales-Cespedes, A. Garcia-Armada, and J. M. H. Elmirghani, "User-centric cell formation for blind interference alignment in optical wireless networks," in *ICC 2021 - IEEE International Conference on Communications*, 2021, pp. 1–7.

[13] H. Sifaou, A. Kammoun, K. Park, and M. Alouini, "Robust transceivers design for multi-stream multi-user MIMO visible light communication," *IEEE Access*, vol. 5, pp. 26 387–26 399, 2017.

[14] H. Marshoud, D. Dawoud, V. M. Kapinas, G. K. Karagiannidis, S. Muhaidat, and B. Sharif, "MU-MIMO precoding for VLC with imperfect CSI," in *2015 4th International Workshop on Optical Wireless Communications (IWOW)*, Sep. 2015, pp. 93–97.

[15] T. V. Pham, H. Le-Minh, and A. T. Pham, "Multi-user visible light communication broadcast channels with zero-forcing precoding," *IEEE Transactions on Communications*, vol. 65, no. 6, pp. 2509–2521, June 2017.

[16] T. Fath and H. Haas, "Performance comparison of MIMO techniques for optical wireless communications in indoor environments," *IEEE Transactions on Communications*, vol. 61, no. 2, pp. 733–742, February 2013.

[17] T. Gou, C. Wang, and S. A. Jafar, "Aiming perfectly in the dark-blind interference alignment through staggered antenna switching," *IEEE Transactions on Signal Processing*, vol. 59, no. 6, pp. 2734–2744, June 2011.

[18] M. Morales-Cespedes, M. C. Paredes-Paredes, A. Garcia-Armada, and L. Vandendorpe, "Aligning the light without channel state information for visible light communications," *IEEE Journal on Selected Areas in Communications*, vol. 36, no. 1, pp. 91–105, Jan 2018.

[19] A. Nuwanpriya, S. Ho, and C. S. Chen, "Indoor MIMO visible light communications: Novel angle diversity receivers for mobile users," *IEEE Journal on Selected Areas in Communications*, vol. 33, no. 9, pp. 1780–1792, Sep. 2015.

[20] C. Chen, M. D. Soltani, M. Safari, A. A. Purwita, X. Wu, and H. Haas, "An omnidirectional user equipment configuration to support mobility in lifi networks," in *2019 IEEE International Conference on Communications Workshops (ICC Workshops)*, 2019, pp. 1–6.

[21] M. Morales-Céspedes, A. A. Quidan, and A. G. Armada, "Experimental evaluation of the reconfigurable photodetector for blind interference alignment in visible light communications," in *2019 27th European Signal Processing Conference (EUSIPCO)*, 2019, pp. 1–5.

[22] L. Xie and X. Zhang, "TDMA and FDMA based resource allocations for quality of service provisioning over wireless relay networks," in *2007 IEEE Wireless Communications and Networking Conference*, March 2007, pp. 3153–3157.

[23] X. Pei, T. Jiang, D. Qu, G. Zhu, and J. Liu, "Radio-resource management and access-control mechanism based on a novel economic model in heterogeneous wireless networks," *IEEE Transactions on Vehicular Technology*, vol. 59, no. 6, pp. 3047–3056, July 2010.

[24] W. Shen and Q. Zeng, "Resource management schemes for multiple traffic in integrated heterogeneous wireless and mobile networks," in *2008 Proceedings of 17th International Conference on Computer Communications and Networks*, Aug 2008, pp. 1–6.

[25] I. Blau, G. Wunder, I. Karla, and R. Sigle, "Decentralized utility maximization in heterogeneous multicell scenarios with interference limited and orthogonal air interfaces," *EURASIP Journal on Wireless Communications and Networking*, vol. 2009, no. 1, p. 104548, Jan 2009.

[26] M. Ismail and W. Zhuang, "A distributed multi-service resource allocation algorithm in heterogeneous wireless access medium," *IEEE Journal*

on Selected Areas in Communications, vol. 30, no. 2, pp. 425–432, February 2012.

[27] C. Gong, S. Li, Q. Gao, and Z. Xu, "Power and rate optimization for visible light communication system with lighting constraints," *IEEE Transactions on Signal Processing*, vol. 63, no. 16, pp. 4245–4256, Aug 2015.

[28] D. Bykhovsky and S. Arnon, "Multiple access resource allocation in visible light communication systems," *Journal of Lightwave Technology*, vol. 32, no. 8, pp. 1594–1600, April 2014.

[29] O. Z. Alsulami, A. A. Alahmadi, S. O. M. Saeed, S. H. Mohamed, T. E. H. El-Gorashi, M. T. Alresheedi, and J. M. H. Elmirghani, "Optimum resource allocation in 6g optical wireless communication systems," in *2020 2nd 6G Wireless Summit (6G SUMMIT)*, 2020, pp. 1–6.

[30] O. Z. Alsulami, A. A. Alahmadi, S. O. M. Saeed, S. H. Mohamed, T. E. H. El-Gorashi, M. T. Alresheedi, and J. M. H. Elmirghani, "Optimum resource allocation in optical wireless systems with energy-efficient fog and cloud architectures," *Phil. Trans. R. Soc. A*, vol. 378, no. 2169, 2020.

[31] O. Z. Alsulami, S. O. M. Saeed, S. H. Mohamed, T. E. H. El-Gorashi, M. T. Alresheedi, and J. M. H. Elmirghani, "Resource allocation in co-existing optical wireless hetnets," in *2020 22nd International Conference on Transparent Optical Networks (ICTON)*, 2020, pp. 1–7.

[32] J. M. Kahn and J. R. Barry, "Wireless infrared communications," *Proceedings of the IEEE*, vol. 85, no. 2, pp. 265–298, Feb 1997.

[33] T. Komine and M. Nakagawa, "Fundamental analysis for visible-light communication system using led lights," *IEEE Transactions on Consumer Electronics*, vol. 50, no. 1, pp. 100–107, Feb 2004.

[34] Q. F. Zhou, A. Huang, M. Peng, F. Qu, and L. Fan, "On the mode switching of reconfigurable-antenna-based blind interference alignment," *IEEE Transactions on Vehicular Technology*, vol. 66, no. 8, pp. 6958–6968, 2017.

[35] T. Gou, S. A. Jafar, and C. Wang, "On the degrees of freedom of finite state compound wireless networks," *IEEE Transactions on Information Theory*, vol. 57, no. 6, pp. 3286–3308, 2011.

[36] L. Bottou and Y. Bengio, "Convergence properties of the K-Means algorithms," in *Advances in Neural Information Processing Systems 7*, G. Tesauro, D. S. Touretzky, and T. K. Leen, Eds. MIT Press, 1995, pp. 585–592.

[37] H. Shen and T. Basar, "Differentiated internet pricing using a hierarchical network game model," in *Proceedings of the 2004 American Control Conference*, vol. 3, June 2004, pp. 2322–2327 vol.3.

[38] S. Stanczak, M. Wiczanowski, and H. Boche, "Fundamentals of resource allocation in wireless networks: Theory and algorithms," in *Springer Verlag*, vol. 3, 2009.

[39] S. H. Low and D. E. Lapsley, "Optimization flow control. I. basic algorithm and convergence," *IEEE/ACM Transactions on Networking*, vol. 7, no. 6, pp. 861–874, Dec 1999.

[40] C. Y. Wong, R. Cheng, K. Lataief, and R. Murch, "Multiuser ofdm with adaptive subcarrier, bit, and power allocation," *IEEE Journal on Selected Areas in Communications*, vol. 17, no. 10, pp. 1747–1758, 1999.

[41] S. Boyd and L. Vandenberghe, "Convex optimization," in *Cambridge University Press*, 2004.

[42] Q. Ye, B. Rong, Y. Chen, M. Al-Shalash, C. Caramanis, and J. G. Andrews, "User association for load balancing in heterogeneous cellular networks," *IEEE Transactions on Wireless Communications*, vol. 12, no. 6, pp. 2706–2716, 2013.

[43] D. Bertsekas, *Convex Optimization Theory*, ser. Athena Scientific optimization and computation series. Athena Scientific, 2009.